ORIGINAL RESEARCH ARTICLE

WILEY *Journal of* Cellular Physiology

Dose- and time-dependent alterations in lipid metabolism after pharmacological PGC-1α activation in L6 myotubes

Elżbieta Supruniuk | Agnieszka Mikłosz [ID] | Adrian Chabowski | Bartłomiej Łukaszuk [ID]

Department of Physiology, Medical University of Bialystok, Bialystok, Poland

Correspondence
Agnieszka Mikłosz, Ph.D., Department of Physiology, Medical University of Bialystok, Mickiewicza 2C Street, 15-222 Bialystok, Poland.
Email: agnieszka.miklosz@umb.edu.pl

Abstract

Pyrroloquinoline quinone (PQQ) acts as a powerful modulator of PGC-1α activation and therefore regulates multiple pathways involved in cellular energy homeostasis. In the present study, we assessed the effects of L6 myotubes incubation with 0.5, 1, and 3 μM PQQ solution for 2 and 24 hr with respect to the cells' lipid metabolism. We demonstrated that PQQ significantly elevates PGC-1α content in a dose- and time-dependent manner with the highest efficiency for 0.5 and 1 μM. The level of free fatty acids was diminished (24 hr: −66%), while an increase in triacylglycerol (TAG) amount was most pronounced after 0.5 μM (2 hr: +93%, 24 hr: +139%) treatment. Ceramide (CER) content was elevated after 2 hr incubation with 0.5 μM and after prolonged exposure to all PQQ concentrations. The cells treated with PQQ for 2 hr exhibited decreased sphinganine (SFA) and sphinganine-1-phosphate (SFA1P) level, while 24 hr incubation resulted in an elevated sphingosine (SFO) amount. In summary, PGC-1α activation promotes TAG and CER synthesis.

KEYWORDS

DAG, FFA, L6 myotubes, PGC-1α, pyrroloquinoline quinone, sphingolipids, TAG

1 | INTRODUCTION

Skeletal muscles constitute ~40% of the total body mass and therefore act as a crucial tissue for plasma lipoprotein-derived fatty acids and free fatty acids (FFA) clearance (Frontera & Ochala, 2015). Despite the relatively high oxidative capacity of this tissue, fatty acids derived from the circulation can contribute to intramyocellular lipid accumulation. The vast majority of FFA (~60%) is channeled into muscular triacylglycerol (TAG) pool, while the rest can be incorporated into other lipid classes, such as diacylglycerols (DAG) or sphingolipids (Watt & Hoy, 2012). Each of these fractions can influence cellular signaling pathways and function. Briefly, TAG was proven to act as a substrate covering myocytes energy requirements, while its increased storage was observed in both insulin resistant and endurance-trained subjects (Sitnick et al., 2013). On the other hand,

abnormal DAG storage was found to enhance the activity of apoptotic molecules (i.e., caspase-3), which induces the progression of skeletal muscle atrophy (Lipina & Hundal, 2017) and impairs insulin signal transduction through the activation of several protein kinase C (PKC) isoforms (Watt & Hoy, 2012).

Recently, sphingolipids have become a subject of great interest and different interventional approaches have been applied to modulate their metabolism. A central molecule of sphingolipid signaling pathway is ceramide (CER). It can accumulate in cells mainly through de novo synthesis from palmitoyl-CoA and serine or through the salvage–recycling pathway from other sphingolipid-derived compounds, such as sphingosine (SFO) and sphingosine-1-phosphate (S1P). Alternatively, CER can be formed through sphingomyelin hydrolysis by alkaline, neutral, or acidic sphingomyelinases (SMase) (Figure 1) (Nikolova-Karakashian & Reid, 2011). It has been acknowledged that
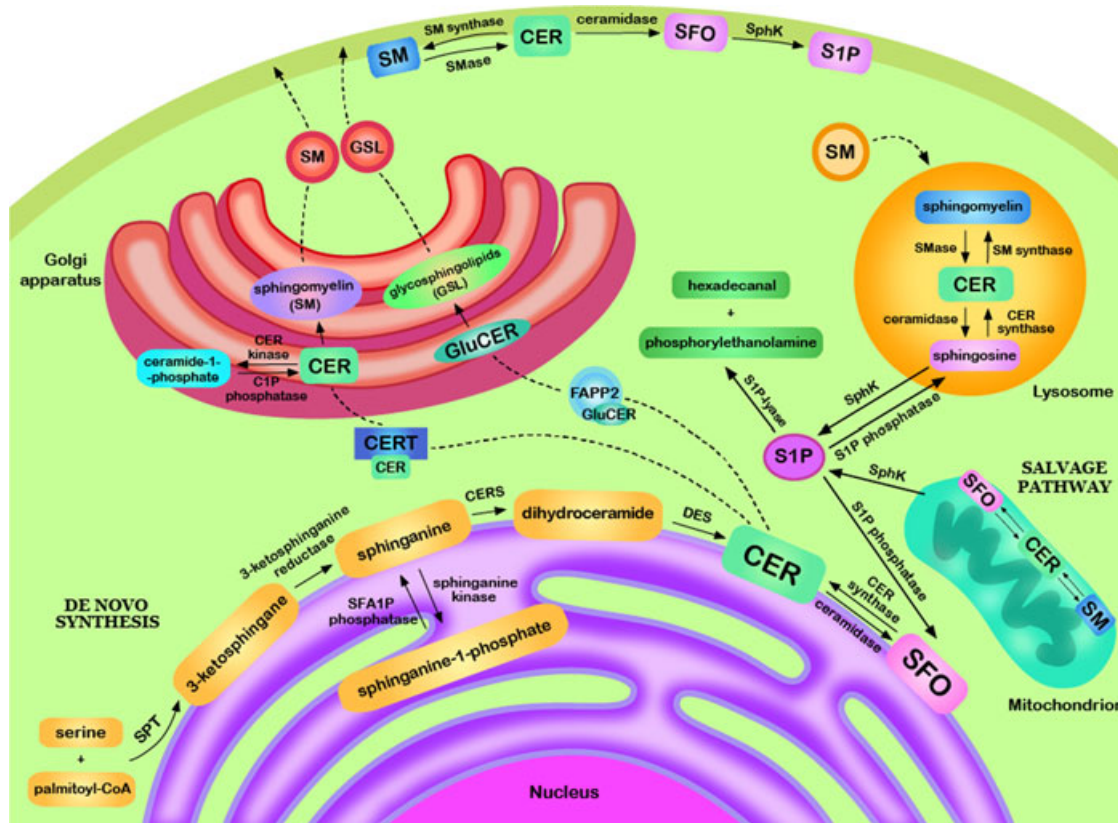
FIGURE 1 Ceramide (CER) synthesis and degradation pathways. De novo synthesis includes the condensation of serine and palmitoyl-CoA through the action of serine palmitoyltransferase (SPT). The product of this reaction, 3-ketosphinganine, is reduced to sphinganine (SFA) by 3-ketosphinganine reductase. SFA can be further converted into sphinganine-1-phosphate (SFA1P) by SFA kinase or can be acylated into dihydroceramide in a reaction catalyzed by ceramide synthases (CERS). Subsequently, dihydroceramide desaturase (DES) reduces dihydroceramide (N-acylsphinganine) to CER. Moreover, CER can be generated through the hydrolysis of membrane and lysosomal sphingomyelin (SM) via alkaline/neutral and acidic sphingomyelinases (SMase), respectively. Additionally, the salvage pathway allows CER formation from sphingosine (SFO) and sphingosine-1-phosphate (S1P). These reactions can be reversed by ceramidase and SFO kinase (SphK). Irreversible degradation of S1P occurs at the endoplasmic reticulum via the action of S1P-lyase [Color figure can be viewed at wileyonlinelibrary.com]

the accumulation of CER contributes to the development of insulin resistance in rodents and humans (Bruni & Donati, 2008). Muscular CER deposition also disturbs mitochondrial structure, diminishes mitochondrial respiration capacity and enhances reactive oxygen species production (Smith et al., 2013).

Peroxisome proliferator-activated receptor (PPAR) γ coactivator 1α (PGC-1α) plays a critical role in the control of gene programs involved in mitochondrial biogenesis and metabolic homeostasis (Supruniuk, Mikłosz & Chabowski, 2017). A positive association between PGC-1α expression and cellular capacity to completely oxidize fatty acids (Hoeks et al., 2012) may serve as a key factor in the reduction of intramuscular lipid accumulation, therefore contributing to an improvement in skeletal muscle insulin sensitivity. Research on transgenic (TG) animals overexpressing PGC-1α revealed that modest upregulation of the coactivator expression is sufficient to improve cellular functions, while its over-excessive level leads to functional and structural anomalies (i.e., lipid overload and extensive mitochondrial proliferation; Choi et al., 2008).

In the present study we used pyrroloquinoline quinone (PQQ) as a means of PGC-1α pharmacological activation. This bioactive compound

was originally identified as a novel coenzyme of several bacterial dehydrogenases. It has been reported that PQQ stimulates mitochondrial biogenesis through CREBP (cAMP response element binding protein) phosphorylation and increased PGC-1α expression (Chowanadisai et al., 2010). However, despite its theoretical therapeutic potential data considering biological role of PQQ are limited and further investigation of the molecule properties is warranted. In our study the initial selection of PQQ doses was based on a thorough analysis of the available literature data. The above-mentioned scrutiny showed that PQQ doses in the range of nanomoles to micromoles are sufficient to exert a significant metabolic effect (Naito, Kumazawa, Kino & Suzuki, 1993). Next, a study of Chowanadisai et al. (2010) demonstrated that Hepa 1–6 cells treated with 10–30 μM of PQQ had notably increased PGC-1α expression, whereas a study by Takada et al. (2012) conducted on muscle cells showed an elevated glucose uptake after their incubation with 100–1,000 nM of PQQ. The above was probably due to the fact that PGC-1α stimulates translocation of glucose transporter, GLUT4, and thus glucose transport itself (Lira, Benton, Yan & Bonen, 2010). Noteworthy, the primary objective of our study was to investigate PQQ/PGC-1α influence on lipid metabolism. Therefore, since fatty acids transport (and

transporters) share a lot of similarities with glucose transport (Samovski, Su, Xu, Abumrad & Stahl, 2012) we considered it (the concentration of 1 μM of PQQ) as a reasonable starting point for our research. Furthermore, while choosing the doses we tried to avoid any toxic effects as evidenced by the literature analysis. He, Nukada, Urakami, and Murphy (2003) for instance, revealed that PQQ concentrations in the range of 50–250 μM may cause death of cell cultures. Importantly, there were no evidence for cellular toxicity in a range of 10–30 μM of PQQ on hepatocytes (Chowanadisai et al., 2010), whereas Takada et al. (2012) investigated the influence of PQQ (only the doses in the range 50–1,000 nM were assessed in the study) on C2C12 myotubes and found no evidence of the cells apoptosis.

The effects of PQQ not only seem to be dependent on its concentration, but also on the duration of PQQ treatment. It was shown that the total uptake of ^{3}H-PQQ in cultured human fibroblasts progressed with incubation time and was the highest after 24 hr reaching 37% of the dose given (Stites et al., 2006). Furthermore, in mice, orally administered ^{14}C-PQQ was rapidly absorbed in the lower intestine (20–90% of a total dose) and excreted within 24 hr (Smidt, Unkefer, Houck & Rucker, 1991). Therefore, generally PQQ does not accumulate in the body and its direct physiological effects should best be assessed within this time frame. As to minimal incubation time required, some authors suggest 1 hr pretreatment with PQQ (Yang et al., 2014) as sufficient to exert its biological activity. However, Harris et al. (2013) determined the human serum level and urinary excretion of PQQ at 2, 4, 8, 24, and 48 hr after an oral administration of a single dose, and revealed that the changes in PQQ abundance paralleled in both materials and reached a peak at ~2–3 hr. Considering the above-mentioned findings, in this study we focused on two incubation times with PQQ, namely 2 and 24 hr.

Since PQQ modulates oxidative cellular capacity via the activation of PGC-1α coactivator, a number of pathways associated with fatty acid metabolism may be affected by the administration of this compound. However, to the best of our knowledge, the possible regulation of lipid content and composition in skeletal muscles by PQQ treatment has not been previously studied. Thus, the aim of our study was to determine the effects of short (2 hr) and prolonged (24 hr) incubation with different doses of PQQ (0.5, 1, and 3 μM) on several prominent cellular lipid fractions content and composition as well as on the expression of key enzymes controlling sphingolipids metabolism pathways in L6 myotubes.

2 | MATERIALS AND METHODS

2.1 | Cell culture

Studies were carried out in a differentiated rat-derived L6 skeletal muscle cells purchased from American Type Culture Collection (ATCC). Myoblasts were incubated at 37°C in humidified atmosphere containing 5% CO_2 in high-glucose Dulbecco's modified Eagle's medium (DMEM; Pan Biotech, Aidenbach, Germany) supplemented with 10% fetal bovine serum (FBS; Thermo Fisher Scientific, Waltham, MA) and 1% antibiotic–antimycotic. At the confluency of approximately 60–80% cells were transferred to DMEM (4.5 g/L glucose) with

2% of horse serum to induce their differentiation into myotubes. After about 8–10 days cells were subjected to experiments (≥90% myoblasts were fused to form elongated myotubes as confirmed by visual inspection using phase-contrast microscopy).

2.2 | Cell treatment

Overexpression of PGC-1α was induced by the incubation of L6 cells with a commercially available PQQ stimulator (Pyrroloquinoline quinone disodium salt; Sigma-Aldrich, St. Louis, MO). PQQ stock solution was prepared in water after heating at 37°C and sonication, and stored at −20°C. Directly before the experiment, stock was dissolved in DMEM to obtain the PQQ concentration of 0.5, 1, and 3 μM. L6 myotubes were starved in serum-free DMEM (w/o glucose) for 3 hr and then cells were treated with the indicated concentrations of PQQ (i.e., 0.5, 1, or 3 μM of PQQ) for 2 or 24 hr.

2.3 | RNA isolation and expression analysis

PGC-1α messenger RNA (mRNA) level was assessed by quantitative real-time polymerase chain reaction (qRT-PCR). The RNA was isolated from L6 myotubes using the RNeasy Plus Mini kit (Qiagen, Hilden, Germany) according to the manufacturer's protocol. Genomic DNA contamination was removed from the samples with the application of DNase (Ambion, Foster City, CA). The quality of RNA was evaluated by measuring the absorbancies at 260 and 280 nm. Reverse transcription of the RNA into complementary DNA (cDNA) was performed using the iScript cDNA Synthesis Kit (Bio-Rad, Hercules, CA). The cDNA amplification was carried out on the Bio-Rad Chromo4 System using the SYBR Green JumpStart Taq Ready Mix (Sigma-Aldrich) and the specific primers (Premier Biosoft, Palo Alto, CA). The simultaneous determination of relative cyclophilin A gene expression was used as endogenous control. Primer sequences: PGC-1α: (a) F: 5′-ACA GAC ACC GCA CAC ATC GC-3′; R: 5′-GCT TCA TAG CTG TCA TAC CTG GGC-3′; (b) F: 5′-ATG AAG CCA ATG AGC ACG AAA GG-3′; R: 5′-ATC ACA CGG CGC TCT TCA ATT GC-3′; (c) F: 5′-TCT CGA CAC AGG TCG TGT TCC C-3′; R: 5′-TTT CGT GCT CAT TGG CTT CAT AGC-3′; cyclophilin A: (a) F: 5′-TGT CTC TTT TCG CCG CTT GCT-3′; R: 5′-CAC CAC CCT GGC ACA TGA ATC C-3′; (b) F: 5′-GTC AAC CCC ACC GTG TTC TTC G-3′; R: 5′-TGT GAA GTC ACC ACC CTG GCA C-3′, (c) F: 5′-AGC ACT GGG GAG AAA GGA TT-3′; R: 5′-AGA TGC CAG GAC CTG TAT GC-3′. For further studies, sequences with the highest efficiency were selected (as underlined). The mRNA levels of target gene was normalized to rat cyclophilin A and calculated according to the Pfaffl method (Pfaffl, 2001). All samples were assayed in duplicate.

2.4 | Western blot analysis

Routine Western blot analysis procedure (Mikłosz et al., 2016; Mikłosz, Łukaszuk, Żendzian-Piotrowska, Kurek, Chabowski, 2016) was applied to determine the protein content of selected compounds (i.e., PGC-1α, SPT1, ASAH1, SPHK1, N-SMase, and Alk-SMase). Briefly, cells were lysed in a radioimmunoprecipitation assay (RIPA; 50 mM Tris-HCl, 150 M NaCl, 1 mM EDTA, 1% NP-40,

0.25% Na-deoxycholate, 1 mM phenylmethylsulfonyl fluoride, 1 µg/ml aprotinin, 1 µg/ml leupeptin, 1 µg/ml pepstatin, 1 mM sodium orthovanadate, 1 mM sodium fluoride) buffer with protease and phosphatase inhibitors (Roche Diagnostics GmbH, Mannheim, Germany) and sonicated for 30 s at 4°C. The total protein concentration was determined by means of bicinchoninic acid (BCA) protein assay kit with bovine serum albumin (BSA) as a standard. Then, the samples were boiled at 95°C for 10 min in a buffer containing 2-mercaptoethanol. The proteins (30 µg) were separated by 10% SDS-PAGE and wet transferred onto polyvinylidene fluoride (PVDF) membranes (0.2 µm pores; Bio-Rad). Next, the membranes were blocked in TTBS buffer (50 mM Tris-HCl, 130 mM NaCl, and 0.05% Tween-20) supplemented with 5% nonfat dry milk or 5% bovine serum albumine for 90 min at room temperature. Thereafter, the membranes were immunoblotted overnight at 4°C with the corresponding primary antibodies in a dilution of 1:1,000. The primary antibodies were purchased from Novus Biologicals (i.e., PGC-1α), Sigma-Aldrich (i.e., SPT1, SPHK1 and ASAH1), Santa Cruz Biotechnology (i.e., N-SMase, Alk-SMase and GAPDH). Subsequently, to detect proteins, anti-rabbit or anti-goat IgG horseradish peroxidase-conjugated secondary antibodies (1:3,000; Santa Cruz Biotechnology, Dallas, TX) were used. The protein bands were visualized using an enhanced chemiluminescence substrate (Thermo Fisher Scientific) and quantified by densitometry (Bio-Rad). Ponceau S staining technique was used to confirm equal protein loading on the blot membrane. The protein expression (expressed in Optical Density Arbitrary Units) was normalized to glyceraldehyde 3-phosphate dehydrogenase (GAPDH) level. Control was set at 100 and the experimental groups were expressed relative to the control.

2.5 | 9,10-[³H]-palmitic acid uptake

Palmitic acid uptake was evaluated according to the Chavez and Summers procedure (Chavez & Summers, 2003). Briefly, L6 myotubes were starved for 3 hr before palmitic acid uptake assessment. Afterward, myotubes were incubated for 20 min with medium containing palmitate and bovine serum albumin (Sigma-Aldrich) complex with the addition of 9,10-[³H]-palmitic acid (1 µCi/ml). After medium removal, the reaction was terminated with ice-cold PBS buffer and subsequently cells were solubilized in 0.05 N NaOH. The resulting fluid was transferred to 5 ml scintillation vials and counted using a Packard TRI-CARB 1900 TR scintillation counter. Radioactivity was normalized concerning protein concentration.

2.6 | Lipid analysis

2.6.1 | Concentration of FFA, DAG, TAG, and CER

Lipid fractions (FFA, DAG, TAG, and CER) were extracted from L6 cells using a Bligh and Dyer method (Bligh & Dyer, 1959). Briefly, samples were transferred into glass tubes containing 2 ml of methanol with 0.01% butylated hydroxytoluene (antioxidant) and

4 ml of chloroform. Moreover, 100 µl of internal standard mixture (heptadecanoic acid, 1,2-diheptadecanoin, and triheptadecanoin; Sigma-Aldrich) was added. After 24 hr, 1.5 ml of water was added to separate lipid layer. Lipids dissolved in chloroform were evaporated under nitrogen stream (37°C) and redissolved in 100 µl of chloroform–methanol solution (2/1, vol/vol). Thereafter, lipids were separated into specific fractions using thin-layer chromatography (TLC; Kieselgel 60, 0.22 mm; Merck, Darmstadt, Germany) with a heptane:isopropyl ether:acetic acid (60:40:3, vol/vol/vol) resolving solution for FFA, DAG, and TAG. CER separation was performed in a solvent containing diethyl ether, hexane, and acetic acid (90:10:1, vol/vol/vol). Dried silica plates were sprayed using 3′7′-dichlorofluorescin (0.2% solution in absolute methanol) and specific bands were visualized under ultraviolet light using standards on the plates. Furthermore, for CER pentadecanoic acid (C15:0; Sigma-Aldrich) was used as an internal standard and transmethylated in 14% boron trifluoride-methanol solution. Similarly, FFA were transmethylated with BF3/methanol (Morrison & Smith, 1964), whereas, DAG fraction was eluted using chloroform–methanol solution (9/1, vol/vol), and eventually an organic phase was redissolved in BF3/methanol solution. Finally, the TAG fraction was eluted and methylated according to Christie (1982). Individual fatty acid methyl esters (FAMEs) in each fraction were identified and quantified according to the retention times of standards by gas–liquid chromatography (Hewlett-Packard 5890 Series II gas chromatograph, HP-INNOWax capillary column; Agilent Technologies, Santa Clara, CA). Total amount of FFA, TAG, DAG and CER was estimated as the sum of the particular fatty acid species and it was expressed in nanomoles per milligram of protein.

2.6.2 | Concentration of sphingomyelin

Cell samples were transferred to a tube containing a solution of methanol and 0.01% butylated hydroxytoluene (Sigma-Aldrich) as an antioxidant. Then, the lipid samples were spotted on TLC silica plates and developed as described by Mahadevappa and Holub (1987). Standards of sphingomyelin (Sigma-Aldrich) were run along with the samples. Lipid bands were visualized under ultraviolet light and the gel bands corresponding to the sphingomyelin were scraped off the plate and transferred into screw tubes containing pentadecanoic acid (Sigma-Aldrich) as an internal standard. Sphingomyelin fatty acids were then transmethylated and subsequently analyzed by means of gas–liquid chromatography. The sphingomyelin content is presented as the sum of individual fatty acid residues.

2.6.3 | Concentration of S1P, SFA1P, SFO, and SFA

The content of selected sphingolipids was determined as described previously in detail (Mikłosz, Łukaszuk, Baranowski, Górski & Chabowski, 2013). Briefly, lipids were extracted from samples in the presence of internal standards (10 pmol of C17-sphingosine and 30 pmol of C17-S1P; Avanti Polar Lipids, Alabaster, AL). The

amount of S1P and SFA1P was evaluated indirectly after dephosphorylation to SFO and SFA, respectively, with the use of alkaline phosphatase (bovine intestinal mucosa; Sigma-Aldrich). Free SFO, SFA, and dephosphorylated sphingoid bases were then converted to their o-phthalaldehyde derivatives and analyzed using a HPLC system (ProStar; Varian Inc., Palo Alto, CA) equipped with a fluorescence detector and C18 reversed-phase column (Varian Inc. OmniSpher 5, 4.6 × 150 mm). The isocratic eluent composition of acetonitrile (Merck, Darmstadt, Germany): water (9:1, vol/vol) and a flow rate of 1 ml/min were used. Column temperature was maintained at 30°C.

2.7 | Data analysis and statistics

The data were analyzed using analysis of variance (ANOVA) and a subsequent post hoc test (pairwise Student's t test). Before the above, the assumptions of the methods, that is normality of the data distribution (Shapiro–Wilk test) and homogenity of variance (Levene's test), were checked. If case they did not hold, nonparametric Kruskall–Wallis test with the following pairwise Wilcoxon test were applied. Additionally, Benjamini–Hochberg multiplicity correction was applied to obtain unbiased p-values (control of the overall type I error). The differences with p values below 0.05 were considered to be statistically significant. Sample size ($n = 6$ per group) was determined based on a previously conducted pilot study (power ≥ 0.8).

3 | RESULTS

3.1 | PQQ upregulates PGC-1α expression in L6 myotubes

First, we evaluated the efficiency of PQQ stimulation on PGC-1α gene and protein expressions in L6 myotubes. As illustrated in Figure 2a, short-term (2 hr) incubation with all PQQ doses caused substantial increases in PGC-1α mRNA level (0.5, 1, 3 μM vs. ctrl: +108%, +123%, +31%, respectively; $p < 0.05$). Similarly, 24 hr exposure to PQQ also induced increases in PGC-1α transcript contents (0.5, 1, 3 μM vs. ctrl: +179%, +208%, +85%, respectively; $p < 0.05$). Additionally, we observed statistically significant differences between both the incubation times (24 hr vs. 2 hr) for 1 and 3 μM of PQQ (+38% and +41%, respectively; $p < 0.05$; Figure 2a). In contrast, western blot analysis revealed significant increases in PGC-1α protein contents only after incubation with 0.5 μM of PQQ (2 hr: +24%; 24 hr: +22%; $p < 0.05$) as compared with the control. We observed no differences in PGC-1α protein expression between the two incubation times (24 hr vs. 2 hr) for any of the applied concentrations (Figure 2b).

3.2 | Palmitic acid uptake in skeletal muscle cells

Basal uptake of palmitic acid was elevated solely in the case of 24 hr incubation with 0.5 μM of PQQ (+36%; $p < 0.05$). Moreover, a marked
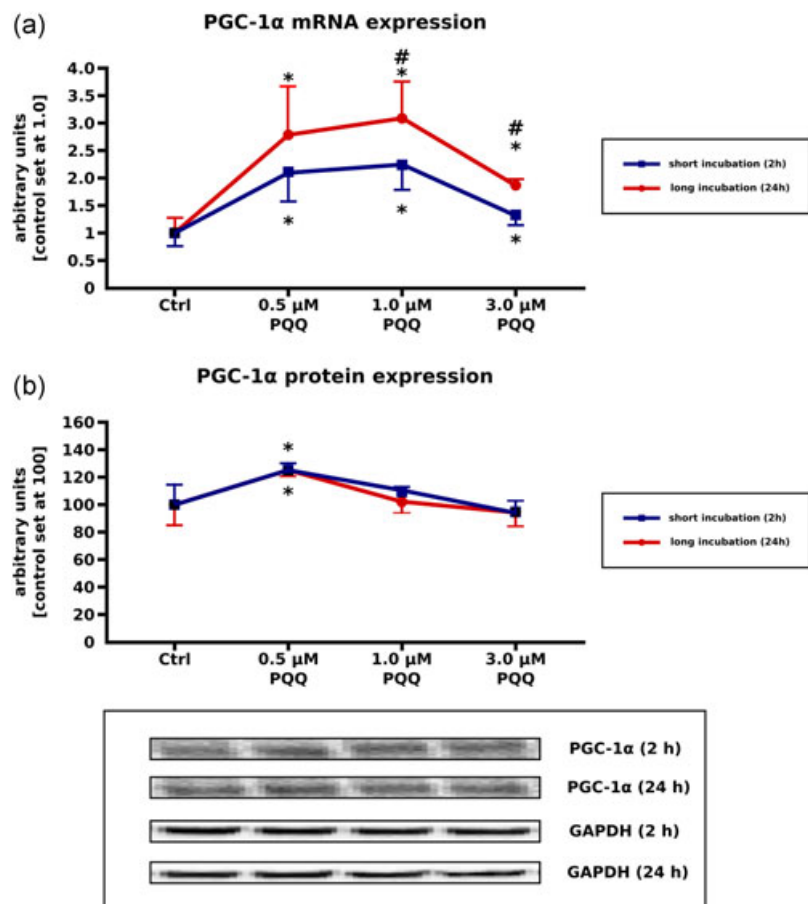
FIGURE 2 Effects of short- and long-time incubation with PQQ on the PGC-1α mRNA (a) and protein levels (b) in L6 myotubes. Measurement of each treatment was taken as the average of six wells in the same experiments. Data are based on three independent determinations. Control is set as 100 (mRNA) or 1 (protein). The values are presented as mean ± SD. ANOVA with post hoc pairwise Student's t test (with Benjamini–Hochberg multiplicity correction). *$p < 0.05$, study group versus control; #$p < 0.05$, long- versus short-time incubation. Error bars (SD) are drawn in opposite directions to avoid overplotting. ANOVA: analysis of variance; mRNA: messenger RNA; PQQ: pyrroloquinoline quinone [Color figure can be viewed at wileyonlinelibrary.com]
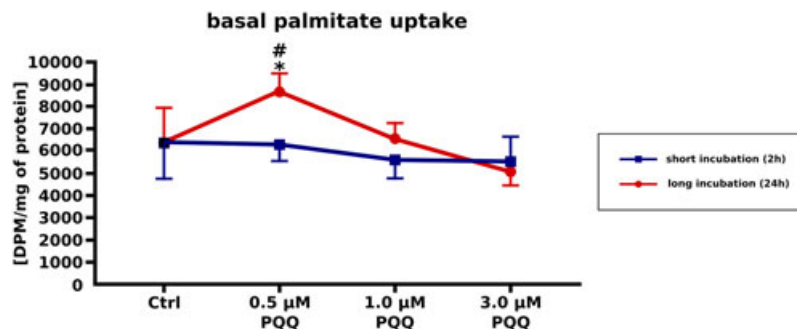
FIGURE 3 Effects of short- and long-time incubation with PQQ on basal palmitic acid uptake in L6 myotubes. Measurement of each treatment was taken as the average of six wells in the same experiments. Data are based on three independent determinations. The values (DPM × mg^{-1} of protein) are presented as mean ± SD. ANOVA with post hoc pairwise Student's _t_ test (with Benjamini–Hochberg multiplicity correction). *$p < 0.05$, study group versus control; #$p < 0.05$, long- versus short-time incubation. Error bars (SD) are drawn in opposite directions to avoid overplotting. ANOVA: analysis of variance; PQQ: pyrroloquinoline quinone [Color figure can be viewed at wileyonlinelibrary.com]

time-dependent difference in palmitate intracellular transport was noticed for this concentration of PQQ (24 hr vs. 2 hr: +37%; $p < 0.05$; Figure 3).

3.3 | The examined lipid fractions content and composition in L6 myotubes

3.3.1 | FFAs content and composition in L6 myotubes

Short-time exposure (2 hr) to 1 μM of PQQ decreased cellular FFA level (−66% vs. ctrl; $p < 0.05$) in L6 cells (Figure 4a) as a consequence of a decline in the content of both saturated (−68% vs. ctrl; $p < 0.05$) and unsaturated fatty acids (−30% vs. ctrl; $p < 0.05$; Table 1). The changes in saturated fatty acids were attributed to a diminishment in palmitic (−68% vs. ctrl; $p < 0.05$), stearic (−74% vs. ctrl; $p < 0.05$) and arachidic acids content (−61% vs. ctrl; $p < 0.05$). Additionally, PQQ-dependent reduction in the amount of unsaturated fatty acids was connected with a decrease in linoleic acid (−57% vs. ctrl; $p < 0.05$).

Prolonged (24 hr) incubation with all the PQQ doses decreased FFA contents in the skeletal muscle cells as compared with control group (0.5, 1, and 3 μM vs. ctrl: −62%, −62%, −74%, respectively; $p < 0.05$; Figure. 4a). Simultaneously, a significant decrease was observed in the content of saturated fatty acids (0.5, 1, 3 μM vs. ctrl: −65%, −65%, −76%, respectively; $p < 0.05$), predominantly myristic (3 μM vs. ctrl: −63%; $p < 0.05$), palmitic (0.5, 1, 3 μM vs. ctrl: −67%, −66%, −76%, respectively; $p < 0.05$), stearic (0.5, 1, 3 μM vs. ctrl: −65%, −69%, −79%, respectively; $p < 0.05$) and arachidic (0.5, 1, 3 μM vs. ctrl: −44%, −61%, −61%, respectively; $p < 0.05$) acids (Table 1). Additionally, in comparison with the control group, PQQ treatment caused a reduction in the amount of unsaturated fatty acids after prolonged PQQ exposure (0.5, 1, 3 μM vs. ctrl: −17%, −28%, −44%, respectively; $p < 0.05$). The above was reflected in a reduction in linoleic (0.5, 1, 3 μM vs. ctrl: −50%, −42%, −69%, respectively; $p < 0.05$), palmitooleic (3 μM vs. ctrl: −27%; $p < 0.05$), oleic (3 μM vs. ctrl: −38%; $p < 0.05$) and linolenic (3 μM vs. ctrl: −46%; $p < 0.05$) acids (Table 1).

Additionally, time-dependent differences in FFA levels were demonstrated for 0.5 and 3 μM of PQQ (24 hr vs. 2 hr; 0.5 μM: −65%; 3 μM: −77%; $p < 0.05$; Figure 4a).

3.3.2 | DAG content and composition in L6 myotubes

Neither prolonged (24 hr), nor short-time treatment (2 hr) with PQQ altered intracellular DAG content, although a substantial difference in the case of time-dependent incubation was shown for 1 μM of PQQ (24 hr vs. 2 hr: +89%; $p < 0.05$; Figure 4b). Furthermore, the concentration of saturated and unsaturated fatty acids remained unaltered (Table 2).

3.3.3 | TAG content and composition in L6 myotubes

TAG level was elevated after short-term incubation with all the studied PQQ doses (0.5, 1, 3 μM vs. ctrl: +93%, +58%, +52%, respectively; $p < 0.05$; Figure 4c). This was accompanied by significant increases in saturated fatty acids level (0.5, 1, 3 μM vs. ctrl: +109%, +61%, +63%, respectively; $p < 0.05$), in particular palmitic (0.5, 1 μM vs. ctrl: +38%, +36%), stearic (0.5, 3 μM vs. ctrl: +292%, +157%; $p < 0.05$), and arachidic (0.5, 1, 3 μM vs. ctrl: +292%, +76%; +51%; $p < 0.05$) acids (Table 3). Furthermore, unsaturated fatty acids amount was increased in the case of short-time treatment with 0.5 and 1 μM of PQQ (2 hr vs. ctrl: +49%, +34%; $p < 0.05$). Specifically, we demonstrated increases in the contents of oleic (0.5, 1 μM vs. ctrl: +59%, +54%, respectively; $p < 0.05$), linoleic (0.5 μM vs. ctrl: +112%; $p < 0.05$) and linolenic (0.5, 1 μM vs. ctrl: +180%, +100%, respectively; $p < 0.05$) acids (Table 3).

Similarly, TAG level was elevated after prolonged exposure to PQQ (0.5, 1, 3 μM vs. ctrl: +139%, +59%, +28%, respectively; $p < 0.05$; Figure 4c). This effect coincided with enhanced levels of saturated fatty acids (0.5, 1, 3 μM vs. ctrl: +161%, +75%, +31%, respectively; $p < 0.05$), specifically palmitic (0.5, 1 μM vs. ctrl: + 126%, +65%; $p < 0.05$), stearic (0.5, 1 μM vs. ctrl: +372%, +76%; $p < 0.05$) and arachidic (0.5 μM vs. ctrl: +372%; $p < 0.05$) acids. Additionally, the content of unsaturated fatty acids increased as a result of long-time
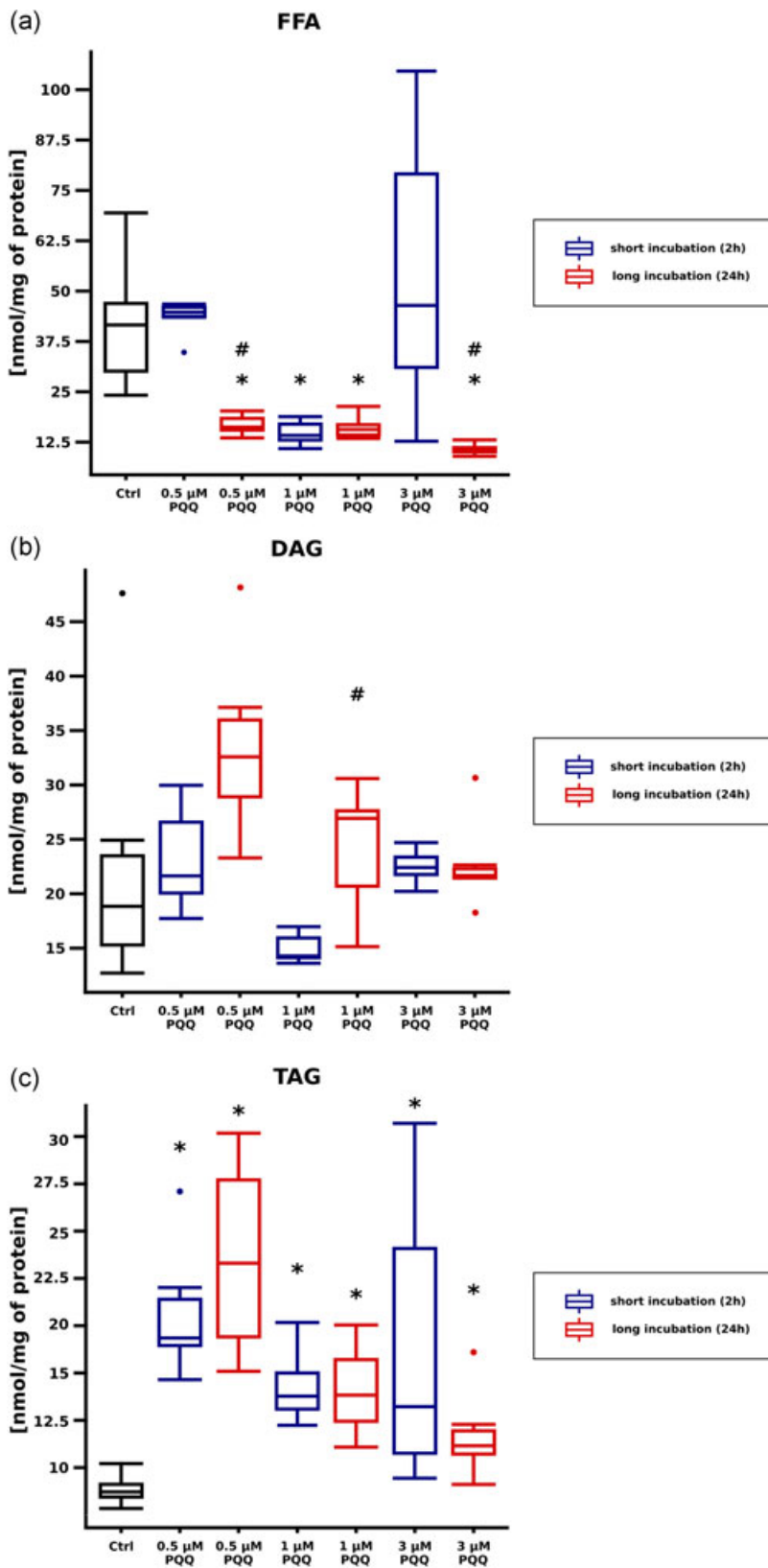
FIGURE 4 Effects of short- and long-term incubation with PQQ on the intracellular content of FFA (a), DAG (b), and TAG (c) in L6 myotubes. Measurement of each treatment was taken as the average of six wells in the same experiments. Data are based on three independent determinations. The values (nmol × mg^{-1} of protein) are expressed as median (25–75%). ANOVA with post hoc pairwise Student's t test (with Benjamini–Hochberg multiplicity correction). *p < 0.05, study group versus control; #p < 0.05, long- versus short-time incubation. ANOVA: analysis of variance; DAG: diacylglycerols; FFA: free fatty acids; PQQ: pyrroloquinoline quinone; TAG: triacylglycerol [Color figure can be viewed at wileyonlinelibrary.com]

TABLE 1 Effects of short- and long-time incubation with PQQ on fatty acids composition of free fatty acids (FFA)

Acid	Control	2 hr PQQ			24 hr PQQ		
		0.5 µM	1 µM	3 µM	0.5 µM	1 µM	3 µM
Myrystic (14:0)	0.98 (0.79–1.22)	1.43 (1.42–1.45)	1.06 (1–1.07)	1.17 (0.93–1.8)	1.26 (1.15–1.38)#	0.97 (0.84–1)	0.36 (0.32–0.44)*#
Palmitic (16:0)	20.11 (14.02–23.12)	21.37 (20.81–21.82)	6.38 (5.5–7.76)*	22.12 (14.51–38.92)	6.69 (6.42–8.29)*#	6.91 (6.17–7.58)*	4.91 (4.48–5.18)*#
Palmitooleic (16:1)	0.33 (0.32–0.35)	0.55 (0.42–0.74)*	0.34 (0.3–0.37)	0.39 (0.3–0.46)	0.38 (0.35–0.4)	0.28 (0.26–0.31)	0.24 (0.23–0.24)*#
Stearic (18:0)	17.57 (12.55–19.9)	17.85 (17.45–19.05)	4.6 (4.12–5.68)*	18.54 (11.68–35.08)	5.38 (4.96–6.18)*#	5.49 (4.91–5.66)*	3.76 (3.47–4.12)*#
Oleic (18:1n9c)	0.77 (0.74–0.84)	1.05 (1.01–1.19)*	0.65 (0.62–0.76)	0.98 (0.78–1.24)	0.67 (0.65–0.69)#	0.59 (0.56–0.66)	0.48 (0.45–0.5)*#
Linoleic (18:2n6c)	0.84 (0.78–0.9)	0.96 (0.94–0.99)	0.36 (0.33–0.37)*	0.94 (0.69–1.58)	0.42 (0.4–0.48)*#	0.49 (0.38–0.57)*	0.26 (0.25–0.27)*#
Arachidic (20:0)	0.18 (0.14–0.2)	0.16 (0.14–0.18)	0.07 (0.06–0.1)*	0.3 (0.17–0.36)	0.1 (0.09–0.12)*	0.1 (0.08–0.11)*	0.07 (0.06–0.07)*#
Linolenic (18n3)	0.13 (0.12–0.15)	0.15 (0.14–0.15)	0.08 (0.08–0.11)	0.19 (0.1–0.24)	0.11 (0.11–0.13)	0.1 (0.08–0.11)	0.07 (0.07–0.08)*
Behenic (22:0)	0.05 (0.04–0.08)	0.06 (0.05–0.06)	0.03 (0.02–0.04)	0.04 (0.04–0.06)	0.11 (0.07–0.12)	0.04 (0.04–0.05)	0.03 (0.03–0.04)
Arachidonic (20:4n6)	0.23 (0.18–0.29)	0.25 (0.24–0.27)	0.2 (0.19–0.21)	0.23 (0.23–0.24)	0.34 (0.3–0.35)#	0.25 (0.24–0.26)#	0.24 (0.23–0.25)
Lignoceric (24:0)	0.25 (0.22–0.26)	0.22 (0.2–0.26)	0.24 (0.21–0.29)	0.28 (0.21–0.36)	0.4 (0.32–0.54)*#	0.26 (0.24–0.29)	0.14 (0.13–0.15)*#
Eicosapentaenoic (20:5n3)	0.12 (0.1–0.13)	0.1 (0.08–0.13)	0.11 (0.1–0.12)	0.13 (0.13–0.14)	0.07 (0.07–0.1)	0.12 (0.12–0.13)	0.1 (0.1–0.11)
SAT	39.07 (27.54–44.68)	41.23 (40.41–42.79)	12.46 (10.99–15.32)*	43.52 (28.24–75.79)	13.8 (13.22–16.52)*#	13.85 (12.21–14.6)*	9.26 (8.52–9.94)*#
UNSAT	2.47 (2.3–2.61)	3.06 (2.81–3.48)	1.73 (1.66–1.98)*	2.92 (2.48–3.62)	2.04 (1.92–2.12)*#	1.79 (1.72–2.01)*	1.39 (1.35–1.41)*#
Total	41.59 (29.78–47.24)	44.83 (43.65–45.75)	14.16 (12.7–17.27)*	46.44 (30.72–79.41)	15.81 (15.18–18.64)*#	15.64 (13.92–17.03)*	10.67 (9.87–11.32)*#

Note. Measurement of each treatment was taken as the average of six wells in the same experiments. Data are based on three independent determinations. The values (nmol × mg^{-1} of protein) are expressed as median (25–75%). Kruskall–Wallis test with post hoc pairwise Wilcoxon test (with Benjamini–Hochberg multiplicity correction). *$p < 0.05$, study group versus control; #$p < 0.05$, long- versus short-time incubation.

TABLE 2 Effects of short- and long-time incubation with PQQ on fatty acids composition of diacylglycerols (DAG)

Acid	2 hr PQQ				24 hr PQQ		
	Control	0.5 µM	1 µM	3 µM	0.5 µM	1 µM	3 µM
Myrystic (14:0)	2.4 (1.96–3.39)	2.8 (2.29–3.38)	1.95 (1.74–2.12)	1.66 (1.62–1.71)	3.42 (2.99–6.35)	2.46 (2.3–2.68)	1.78 (1.53–1.94)
Palmitic (16:0)	7.61 (5.95–9.76)	8.59 (7.49–10.97)	5.1 (4.89–5.88)	9.43 (9.02–9.93)	13.21 (10.8–16.18)	11.24 (7.97–11.76)[#]	9.2 (8.73–9.5)
Palmitooleic (16:1)	0.44 (0.4–0.53)	0.79 (0.7–0.86)	0.67 (0.48–0.72)	0.7 (0.65–0.77)	1.13 (0.8–1.33)	0.67 (0.62–1.06)	0.45 (0.36–0.7)
Stearic (18:0)	6.44 (4.72–7.09)	6.24 (5.83–7.04)	4.23 (4.21–4.8)	8.1 (7.57–8.48)	8.47 (8.26–9.75)	8.99 (5.67–9.36)[#]	7.69 (7.52–8.07)
Oleic (18:1n9c)	0.88 (0.69–0.89)	0.99 (0.96–1.02)	0.77 (0.74–0.9)	0.89 (0.83–0.97)	1.25 (1.07–1.32)	1.11 (0.98–1.27)	0.9 (0.76–1.25)
Linoleic (18:2n6c)	0.41 (0.31–0.51)	0.52 (0.51–0.54)	0.39 (0.37–0.4)	0.62 (0.61–0.62)	0.62 (0.54–0.72)	0.65 (0.53–0.69)[#]	0.53 (0.51–0.55)
Arachidic (20:0)	0.08 (0.08–0.11)	0.1 (0.09–0.1)	0.07 (0.07–0.08)	0.11 (0.09–0.12)	0.12 (0.12–0.16)	0.13 (0.13–0.16)	0.13 (0.1–0.14)
Linolenic (18n3)	0.07 (0.06–0.07)	0.06 (0.06–0.07)	0.06 (0.06–0.08)	0.07 (0.06–0.07)	0.13 (0.11–0.18)	0.09 (0.08–0.09)	0.08 (0.06–0.09)
Behenic (22:0)	0.04 (0.04–0.05)	0.05 (0.04–0.06)	0.04 (0.03–0.06)	0.06 (0.05–0.06)	0.06 (0.02–0.07)	0.06 (0.06–0.08)	0.06 (0.06–0.07)
Arachidonic (20:4n6)	0.56 (0.55–0.58)	0.67 (0.66–0.69)	0.75 (0.68–0.79)	0.61 (0.57–0.64)	0.84 (0.7–0.95)	0.65 (0.62–0.68)*	0.69 (0.63–0.75)*
Lignoceric (24:0)	0.14 (0.11–0.18)	0.36 (0.35–0.39)*	0.18 (0.14–0.2)	0.18 (0.15–0.19)	0.49 (0.43–0.52)*	0.24 (0.19–0.26)*	0.16 (0.15–0.17)
Eicosapentaenoic (20:5n3)	0.11 (0.09–0.11)	0.19 (0.17–0.19)*	0.1 (0.09–0.11)	0.14 (0.13–0.15)*	0.19 (0.17–0.23)*	0.14 (0.12–0.15)[#]	0.12 (0.11–0.13)[#]
Docosahexaenoic (22:6n3)	ND	ND	0.07 (0.05–0.09)*	ND	ND	ND	ND
SAT	16.18 (13.23–20.08)	18.44 (16.54–23.51)	11.32 (11.24–12.84)	19.57 (18.61–20.53)	28.49 (24.49–28.69)	23.16 (16.6–24.3)	18.94 (18.48–18.97)
UNSAT	2.57 (2.18–2.75)	3.21 (3.18–3.29)	2.76 (2.46–3.1)	3.07 (2.99–3.11)	4.36 (4–4.45)	3.36 (3.31–3.9)	3.04 (2.58–3.48)
Total	18.85 (15.3–23.49)	21.64 (19.95–26.7)	14.28 (14.02–16.04)	22.42 (21.66–23.46)	32.58 (28.79–36.09)	26.93 (20.58–27.73)[#]	21.68 (21.4–22.41)

Note. Measurement of each treatment was taken as the average of six wells in the same experiments. Data are based on three independent determinations. The values (nmol × mg^{-1} of protein) are expressed as median (25–75%). Kruskall–Wallis test with post hoc pairwise Wilcoxon test (with Benjamini–Hochberg multiplicity correction). *$p < 0.05$, study group versus control; #$p < 0.05$, long- versus short-time incubation.

TABLE 3 Effects of short- and long-time incubation with PQQ on fatty acids composition of triacylglycerols (TAG)

Acid	Control	2 hr PQQ			24 hr PQQ		
		0.5 μM	1 μM	3 μM	0.5 μM	1 μM	3 μM
Myristic (14:0)	1.14 (1.01–1.16)	1.56 (1.3–2.04)	1.2 (1.14–1.25)	1.17 (1.04–1.8)	1.73 (1.41–1.86)	1.48 (1.41–1.55)	1.33 (1.3–1.38)
Palmitic (16:0)	2.44 (2.34–2.68)	3.37 (3.06–3.68)*	3.32 (3.16–3.68)*	3.71 (2.93–6.06)	5.52 (4.46–6.86)*	4.03 (3.37–5.18)*	3.32 (3.09–4.18)
Palmitoleic (16:1)	0.88 (0.72–1.02)	1.04 (1.02–1.09)	1.07 (1–1.08)	0.75 (0.62–1.22)	1.21 (1.09–1.41)	0.88 (0.86–0.97)	0.83 (0.81–0.96)
Stearic (18:0)	1.05 (1–1.38)	2.17 (2.09–2.26)*	2.1 (1.86–2.34)*	2.7 (2.23–5.58)*	2.84 (2.6–3.27)*#	2.48 (2.27–2.55)*	1.53 (1.29–1.82)
Oleic (18:1n9c)	1.14 (0.98–1.28)	1.81 (1.8–1.89)*	1.76 (1.56–1.95)*	1.42 (1.13–1.61)	1.86 (1.68–2.97)*	1.54 (1.45–1.65)*	1.15 (1.03–1.33)
Linoleic (18:2n6c)	0.43 (0.41–0.44)	0.91 (0.83–1.04)*	0.52 (0.49–0.55)	0.54 (0.52–0.58)	0.84 (0.55–1.8)*	0.5 (0.47–0.91)	0.48 (0.41–0.53)
Arachidic (20:0)	0.74 (0.34–0.86)	2.9 (2.44–4.31)*	1.3 (1.14–5.18)*	1.12 (0.87–1.79)*	3.49 (1.8–3.93)*	0.93 (0.9–0.94)	0.78 (0.78–0.8)
Linolenic (18n3)	0.1 (0.08–0.11)	0.28 (0.2–0.3)*	0.2 (0.16–0.27)*	0.25 (0.18–0.27)	0.27 (0.2–0.4)	0.18 (0.13–0.23)	0.11 (0.1–0.15)
Behenic (22:0)	0.13 (0.11–0.14)	0.29 (0.25–0.32)*	0.26 (0.2–0.32)*	0.19 (0.18–0.42)	0.44 (0.31–0.51)*	0.28 (0.27–0.29)*	0.18 (0.16–0.2)
Arachidonic (20:4n6)	0.22 (0.16–0.29)	0.21 (0.15–0.29)	0.33 (0.28–0.43)	0.3 (0.26–0.44)	0.36 (0.3–0.96)	0.3 (0.27–0.37)	0.28 (0.25–0.29)
Lignoceric (24:0)	0.27 (0.22–0.29)	1.42 (1.25–1.68)*	0.28 (0.23–0.34)	0.59 (0.49–1.1)*	0.68 (0.5–0.88)*#	0.38 (0.24–0.46)	0.36 (0.32–0.44)*#
Eicosapentaenoic (20:5n3)	0.17 (0.15–0.19)	0.39 (0.32–0.47)*	0.16 (0.15–0.17)	0.21 (0.13–0.31)	0.44 (0.39–0.53)*	0.16 (0.13–0.23)	0.21 (0.18–0.25)
Nervonic (24:1)	0.08 (0.06–0.08)	ND	0.09 (0.09–0.11)	0.24 (0.12–0.35)*	0 (0–0.32)	0.15 (0.12–0.2)	0.13 (0.12–0.13)*
Docosahexaenoic (22:6n3)	ND	0.04 (0.01–0.14)	ND	ND	0.06 (0.01–0.13)	ND	0.1 (0.02–0.14)
SAT	5.83 (5.51–6.12)	12.17 (11.98–14)*	9.39 (8.63–11.5)*	9.48 (7.83–16.57)*	15.24 (12.25–16.68)*	10.22 (8.55–10.85)*	7.66 (7.27–7.97)*
UNSAT	3.15 (2.59–3.33)	4.68 (4.35–5.03)*	4.21 (4.01–4.35)*	3.75 (2.94–5.07)	5.56 (4.84–8.6)*	3.88 (3.52–4.96)	3.36 (3.12–3.77)
Total	8.72 (8.38–9.18)	16.87 (16.38–18.96)*	13.78 (13.01–15.07)*	13.22 (10.69–21.64)*	20.8 (16.91–25.27)*	13.83 (12.38–15.77)*	11.15 (10.65–12.01)*

Note. Measurement of each treatment was taken as the average of six wells in the same experiments. Data are based on three independent determinations. The values (nmol $\times$ mg^{-1} of protein) are expressed as median (25–75%). Kruskall–Wallis test with post hoc pairwise Wilcoxon test (with Benjamini–Hochberg multiplicity correction).*$p < 0.05$, study group versus control;.*$p < 0.05$, long- versus short-time incubation.
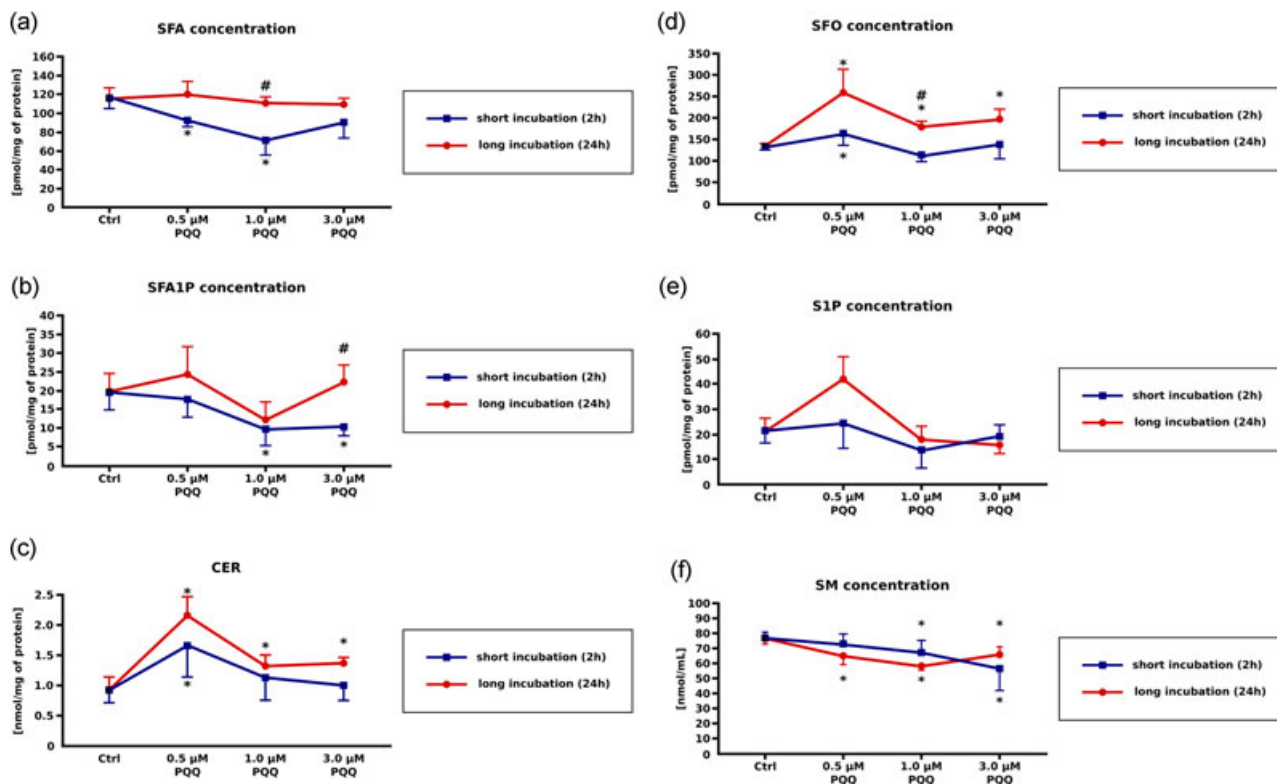
FIGURE 5 Effects of short- and long-term incubation with PQQ on intracellular sphingolipid content: SFA (a), SFA1P (b), CER (c), SFO (d), S1P (e), and sphingomyelin (f) in L6 myotubes. Measurement of each treatment was taken as the average of six wells in the same experiments. Data are based on three independent determinations. The values are presented as mean ± *SD*. ANOVA with post hoc pairwise Student's *t* test (with Benjamini–Hochberg multiplicity correction). *$p < 0.05$, study group versus control; #$p < 0.05$, long- vs. short-time incubation. Error bars (*SD*) are drawn in opposite directions to avoid overplotting. ANOVA: analysis of variance; CER: ceramide; SFA: sphinganine; SFA1P: sphinganine-1-phosphate; SFO: sphingosine; S1P: sphingosine-1-phosphate [Color figure can be viewed at wileyonlinelibrary.com]

exposure to 0.5 μM of PQQ (24 hr vs. ctrl: +77%; $p < 0.05$). In particular, we noticed an increase in the myocellular level of oleic (0.5, 1 μM vs. ctrl: + 63%, +35%, respectively; $p < 0.05$) and linoleic (0.5 μM vs. ctrl: +95%; $p < 0.05$) acids (Table 3).

3.4 | Intracellular sphingolipids content in L6 myotubes

3.4.1 | Sphinganine concentration in L6 myotubes

Short-time (2 hr) incubation with 0.5 and 1 μM of PQQ significantly declined sphinganine (SFA) levels (0.5, 1 μM vs. ctrl: −21% and −40%, respectively; $p < 0.05$) (Figure 5a). On the contrary, prolonged (24 hr) PQQ treatment did not evoke any significant changes in SFA cellular level in comparison with the control cells. Additionally, time-dependent differences in SFA level were noticed for 1 μM PQQ concentration (24 hr vs. 2 hr: +59%; $p < 0.05$; Figure 5a).

3.4.2 | Sphinganine-1-phosphate (SFA1P) concentration in L6 myotubes

A significant drop in SFA1P level was observed after short-time exposure to 1 and 3 μM of PQQ (−50%, −46% versus ctrl, respectively; $p < 0.05$). Simultaneously, a substantial time-dependent

difference was noticed for 3 μM PQQ incubation (24 hr vs. 2 hr: +111%; $p < 0.05$; Figure 5b).

3.4.3 | CER concentration in L6 myotubes

The cells treated with PQQ exhibited increased contents of CER (Figure 5c). In the case of 2 hr incubation, this reached statistical significance level for 0.5 μM of PQQ (+79% vs. ctrl; $p < 0.05$). Simultaneously, the levels of palmitic, arachidic, and behenic acids were elevated (+82%, +75%, +67%, respectively; $p < 0.05$), although the increase in total content of saturated fatty acids was not significant due to high variability (+70%; $p > 0.05$; Table 4). Furthermore, the enhanced content of unsaturated fatty acids (2 hr; 0.5 μM vs. ctrl: +119%; $p < 0.05$) resulted from increased levels of palmitooleic, oleic, linoleic, linolenic, and arachidonic acids (+112.5%, +168%, +267%, +300%, +60%, respectively; $p < 0.05$). The increase in linolenic acid was also noticed after exposure to 1 and 3 μM of PQQ (2 hr; 1, 3 μM vs. ctrl: +167%, +100%, respectively; $p < 0.05$; Table 4).

Prolonged (24 hr) incubation with all doses of PQQ also considerably enhanced CER amount (0.5, 1, 3 μM vs. ctrl: +132%, +41%, +48%, respectively; $p < 0.05$; Figure 5c). The concurrent increase in saturated fatty acids (0.5, 1, 3 μM vs. ctrl: +136%, +50%,

TABLE 4 Effects of short- and long-time incubation with PQQ on fatty acids composition of ceramide (CER)

Acid	2 hr PQQ				24 hr PQQ		
	Control	0.5 µM	1 µM	3 µM	0.5 µM	1 µM	3 µM
Myristic (14:0)	0.207 ± 0.0602	0.326 ± 0.1166	0.228 ± 0.0882	0.252 ± 0.0773	0.499 ± 0.0875*#	0.344 ± 0.0399*#	0.411 ± 0.0267*#
Palmitic (16:0)	0.307 ± 0.1055	0.558 ± 0.1677	0.424 ± 0.1593	0.408 ± 0.1394	0.792 ± 0.2031*	0.489 ± 0.0745	0.464 ± 0.0213
Palmitooleic (16:1)	0.016 ± 0.0019	0.034 ± 0.0116*	0.022 ± 0.0084	0.017 ± 0.007	0.036 ± 0.0049*	0.027 ± 0.0028*	0.035 ± 0.0041*#
Stearic (18:0)	0.216 ± 0.0721	0.365 ± 0.1594	0.247 ± 0.0844	0.194 ± 0.0612	0.413 ± 0.0554*	0.265 ± 0.0521	0.285 ± 0.0358#
Oleic (18:1n9c)	0.068 ± 0.0118	0.182 ± 0.0571*	0.085 ± 0.0262	0.061 ± 0.0228	0.099 ± 0.015*#	0.045 ± 0.0071*#	0.048 ± 0.0059*
Linoleic (C18:2)	0.003 ± 0.0009	0.011 ± 0.0016*	0.002 ± 0.0006	0.005 ± 0.0006*	0.005 ± 0.0015*#	0.007 ± 0.0012*#	0.008 ± 0.001*#
Arachidic (20:0)	0.008 ± 0.0024	0.014 ± 0.0029*	0.01 ± 0.0036	0.01 ± 0.0033	0.021 ± 0.0042*#	0.013 ± 0.0023*	0.016 ± 0.0012*#
Linolenic (C18n3)	0.003 ± 0.0007	0.012 ± 0.0039*	0.008 ± 0.003*	0.006 ± 0.002*	0.006 ± 0.0036	0.01 ± 0.0017*	0.01 ± 0.0014*#
Behenic (22:0)	0.015 ± 0.0029	0.025 ± 0.008*	0.02 ± 0.0073	0.019 ± 0.0056	0.045 ± 0.0058*#	0.019 ± 0.003	0.014 ± 0.0024
Arachidonic (20:4n6)	0.01 ± 0.002	0.016 ± 0.0046*	0.011 ± 0.0036	0.012 ± 0.0032	0.025 ± 0.0036*#	0.012 ± 0.0009	0.014 ± 0.0016*
Lignoceric (24:0)	0.018 ± 0.005	0.025 ± 0.0088	0.016 ± 0.0044	0.021 ± 0.0069	0.048 ± 0.0077*#	0.026 ± 0.0039#	0.023 ± 0.0014
Eicosapentaenoic (20:5n3)	0.014 ± 0.0032	0.021 ± 0.0066	0.019 ± 0.0058	0.02 ± 0.0059	0.036 ± 0.0056*#	0.018 ± 0.0032	0.013 ± 0.0015#
Nervonic (24:1)	0.031 ± 0.0062	0.047 ± 0.0188	0.034 ± 0.0107	0.044 ± 0.0161	0.089 ± 0.0127*#	0.026 ± 0.0038	0.021 ± 0.0022*#
Docosahexaenoic (22:6n3)	0.013 ± 0.0043	0.021 ± 0.007	0.016 ± 0.0041	0.018 ± 0.004	0.038 ± 0.0076*#	0.012 ± 0.0019	0.012 ± 0.0015#
SAT	0.771 ± 0.1972	1.314 ± 0.4489	0.944 ± 0.3418	0.905 ± 0.2863	1.818 ± 0.2916*	1.156 ± 0.1583*	1.212 ± 0.0646*
UNSAT	0.157 ± 0.0241	0.344 ± 0.1037*	0.196 ± 0.0599	0.182 ± 0.0569	0.333 ± 0.0344*	0.157 ± 0.0179	0.161 ± 0.0122
Total	0.928 ± 0.2178	1.658 ± 0.5511*	1.14 ± 0.3993	1.087 ± 0.3398	2.151 ± 0.3103*	1.312 ± 0.1754*	1.373 ± 0.0724*

Note. Measurement of each treatment was taken as the average of six wells in the same experiments. Data are based on three independent determinations. The values (nmol × mg^{-1} of protein) are expressed as mean ± SD. ANOVA with post hoc pairwise Student's *t* test (with Benjamini–Hochberg multiplicity correction). *$p < 0.05$, study group versus control; #$p < 0.05$, long- versus short-time incubation. ANOVA: analysis of variance; PQQ: pyrroloquinoline quinone.

+57%, respectively; $p < 0.05$) was connected with the upregulation of myristic (0.5, 1, 3 µM vs. ctrl: +141%, +66%, +99%, respectively; $p < 0.05$) and arachidic acids (0.5, 1, 3 µM vs. ctrl: + 162.5%, +62.5%, +100%, respectively; $p < 0.05$). Additionally, the level of palmitic, stearic, behenic, and lignoceric acids rose with 0.5 µM of PQQ (+158%, +91%, +200%, +167%, respectively; $p < 0.05$; Table 4). The pronounced effect on unsaturated fatty acids was demonstrated with 0.5 µM of PQQ (+112%; $p < 0.05$) together with elevated content of palmitooleic, oleic, linoleic, arachidonic, eicosapentaenoic, nervonic, and docosahexaenoic acids (+125%, +46%, +67%, +150%, +157%, +187%, +192%, respectively; $p < 0.05$). Despite no changes in total amount of unsaturated fatty acids upon exposure to 1 and 3 µM of PQQ, marked alterations were observed in regard to palmitooleic (1, 3 µM vs. ctrl: +69%, +119%, respectively; $p < 0.05$), oleic (1, 3 µM vs. ctrl: −34%, −29%, respectively; $p < 0.05$), linoleic (1, 3 µM vs. ctrl: +150%, +177%, respectively; $p < 0.05$), linolenic (1, 3 µM vs. ctrl: +233%, +233%, respectively; $p < 0.05$) and arachidonic (3 µM vs. ctrl: +40%, respectively; $p < 0.05$) acids levels (Table 4).

3.4.4 | Sphingosine concentration in L6 myotubes

Prolonged (24 hr) incubation with all the studied PQQ doses resulted in considerable increases in SFO content, namely 0.5 µM enhanced the amount of SFO by 94%, 1 µM by 35%, and 3 µM PQQ by 48% as compared with the control cells ($p < 0.05$; Figure 5d). Interestingly, short-time exposure also resulted in the elevation of SFO level, but only for 0.5 µM of PQQ incubation (+24%; $p < 0.05$). Additionally, for

1 µM of PQQ we noticed a significant difference between 24 and 2 hr incubation times (+58%; $p < 0.05$; Figure 5d).

3.4.5 | S1P concentration in L6 myotubes

We observed an increase by 96% in S1P content after prolonged (24 hr) treatment with 0.5 µM of PQQ, however, due to high variance, it did not reach the statistical significance level ($p > 0.05$; Figure 5e). Similarly, there was a difference between both the incubation times (24 hr vs. 2 hr: +73%) for 0.5 µM of PQQ, although again it did not reach the statistical significance level ($p > 0.05$; Figure 5e).

3.4.6 | Sphingomyelin concentration in L6 myotubes

Short-time incubation decreased sphingomyelin (SM) level in the case of 1 and 3 µM of PQQ (1, 3 µM vs. ctrl: −13%, −27%, respectively; $p < 0.05$; Figure 5f). The analysis of fatty acid composition in this fraction revealed statistically significant decrease in saturated fatty acids contents (1, 3 µM vs. ctrl: −16%, −28%, respectively; $p < 0.05$). This effect ensued predominantly from the observed decline in myristic (3 µM vs. ctrl: −35%; $p < 0.05$), palmitic (1, 3 µM vs. ctrl: −18%, −28%, respectively; $p < 0.05$) and stearic (3 µM vs. ctrl: −26%; $p < 0.05$) acids levels. On the other hand, the concentration of unsaturated fatty acids declined after 2 hr treatment with 3 µM (−19%; $p < 0.05$), although solely a decrease in nervonic acid achieved statistical significance (−24%; $p < 0.05$; Table 5).

TABLE 5 Effects of short- and long-time incubation with PQQ on fatty acids composition of sphingomyelin. Measurement of each treatment was taken as the average of six wells in the same experiments

Acid	Control	2 hr PQQ			24 hr PQQ		
		0.5 µM	1 µM	3 µM	0.5 µM	1 µM	3 µM
Myrystic (14:0)	4.3 ± 0.553	3.99 ± 0.912	3.5 ± 0.415	2.78 ± 0.738*	3.29 ± 1.21	3.13 ± 0.548*	3.45 ± 0.741
Palmitic (16:0)	48.89 ± 3.092	46.85 ± 3.656	40.33 ± 4.536*	34.96 ± 11.597*	40.11 ± 4.251*	36.68 ± 2.12*	40.77 ± 3.52*
Palmitooleic (16:1)	1.07 ± 0.222	0.94 ± 0.306	1.4 ± 1.368	0.82 ± 0.106	0.89 ± 0.137	0.8 ± 0.169	0.94 ± 0.295
Stearic (18:0)	10.64 ± 1.186	10.58 ± 1.13	8.83 ± 1.355	7.87 ± 1.153*	10.76 ± 1.547	7.41 ± 0.645*#	9.57 ± 1.846
Oleic (18:1n9c)	2.35 ± 0.314	2.4 ± 0.602	2.83 ± 1.302	2.02 ± 0.234	2.35 ± 0.099	2.05 ± 0.15	2.17 ± 0.308
Arachidic (20:0)	0.77 ± 0.079	0.37 ± 0.162*	0.67 ± 0.083	0.59 ± 0.141	0.56 ± 0.181	0.58 ± 0.061*	0.66 ± 0.04
Linolenic (C18n3)	0.23 ± 0.07	0.14 ± 0.069	0.21 ± 0.088	0.18 ± 0.025	0.17 ± 0.054	0.18 ± 0.052	0.17 ± 0.012
Behenic (22:0)	1.4 ± 0.132	1.35 ± 0.104	1.35 ± 0.251	1.18 ± 0.204	1.19 ± 0.092	1.21 ± 0.079	1.22 ± 0.081
Arachidonic (20:4n6)	0.44 ± 0.057	0.44 ± 0.105	0.39 ± 0.034	0.38 ± 0.045	0.4 ± 0.055	0.36 ± 0.051	0.39 ± 0.035
Lignoceric (24:0)	0.78 ± 0.05	0.7 ± 0.084	1.68 ± 2.371	0.73 ± 0.068	0.72 ± 0.081	0.69 ± 0.162	0.74 ± 0.06
Eicosapentaenoic (20:5n3)	1.21 ± 0.298	1.14 ± 0.181	1.35 ± 0.908	1.01 ± 0.205	0.95 ± 0.076*	1.03 ± 0.144	1.02 ± 0.072
Nervonic (24:1)	4.15 ± 0.281	3.6 ± 0.935	3.63 ± 0.37*	3.15 ± 0.67*	3.15 ± 0.521*	3.31 ± 0.174*	3.62 ± 0.19*
Docosahexaenoic (22:6n3)	0.86 ± 0.096	0.76 ± 0.098	0.82 ± 0.078	0.76 ± 0.086	0.75 ± 0.077	0.81 ± 0.05	0.86 ± 0.122
SAT	66.78 ± 3.996	63.84 ± 5.04	56.37 ± 6.317*	48.11 ± 13.75*	56.63 ± 5.605*	49.7 ± 2.587*	56.4 ± 5.236*
UNSAT	10.32 ± 0.806	9.42 ± 1.862	10.68 ± 3.442	8.31 ± 1.191*	8.66 ± 0.71*	8.54 ± 0.468*	9.18 ± 0.735
Total	77.11 ± 4.362	73.26 ± 5.973	67.04 ± 8.632*	56.42 ± 14.908*	65.3 ± 6.032*	58.24 ± 2.716*	65.58 ± 5.828*

Note. Measurement of each treatment was taken as the average of six wells in the same experiments. Data are based on three independent determinations. The values (nmol × mg^{-1} of protein) are expressed as mean ± SD. ANOVA with post hoc pairwise Student's t test (with Benjamini–Hochberg multiplicity correction).*$p < 0.05$, study group vs. control; #$p < 0.05$, long- vs. short-time incubation.
PQQ: pyrroloquinoline quinone.

Prolonged (24 hr) treatment with all the tested PQQ concentrations diminished SM contents (0.5, 1, 3 µM vs. ctrl: −15%, −24%, −15%, respectively; $p < 0.05$; Figure 5f) together with a decline in the level of saturated fatty acids (0.5, 1, 3 µM vs. ctrl: −15%, −26%, −16%, respectively; $p < 0.05$). In particular, we revealed a decrease in palmitic (0.5, 1, 3 µM vs. ctrl: −18%, −25%, −17%, respectively; $p < 0.05$), stearic (1 µM vs. ctrl: −30%; $p < 0.05$), myristic (1 µM vs. ctrl: −27%; $p < 0.05$) and arachidic (1 µM vs. ctrl: −25%; $p < 0.05$) acids amount. Moreover, the level of unsaturated fatty acids was diminished after long-term treatment with 0.5 and 1 µM of PQQ (0.5, 1 µM vs. ctrl: −16%, −17%, respectively; $p < 0.05$), while as regards to fatty acid composition, statistical decrease was achieved for nervonic (0.5, 1, 3 µM vs. ctrl: −24%, −20%, −13%, respectively; $p < 0.05$) and eicosapentaenoic acids (0.5 µM vs. ctrl: −22%; $p < 0.05$; Table 5).

3.5 | Protein expression of sphingolipid metabolizing enzymes

Serine palmitoyltransferase 1 (SPT1) protein levels were increased after short (2 hr) and long-time (24 hr) incubation with 0.5 µM (2 hr vs. ctrl: +27%, 24 hr vs. ctrl: +34%; $p < 0.05$) and 1 µM of PQQ (2 hr vs. ctrl: +35%, 24 hr vs. ctrl: +29%; $p < 0.05$). Moreover, we observed a significant difference in SPT1 level between both the incubation times for 3 µM of PQQ (24 hr vs. 2 hr: −18%; $p < 0.05$; Figure 6a).

In the current study we did not observe any significant differences in acidic ceramidase (ASAH1) or sphingosine kinase 1 (SphK1) protein levels neither with respect to PQQ exposure time nor its concentration (Figure 6b,c).

The protein level of neutral sphingomyelinase (N-SMase) was decreased after 2 hr exposure to 3 µM of PQQ (−18% vs. ctrl; $p < 0.05$), although there were no significant alterations in the other conditions. Consequently, time-dependent differences in N-SMase level were observed only in the case of 3 µM of PQQ (24 hr vs. 2 hr: +9%; $p < 0.05$; Figure 6d). Furthermore, there were no significant changes in alkaline sphingomyelinase (Alk-SMase) protein contents (Figure 6e).

4 | DISCUSSION

Exogenously administered PQQ is distributed within various cellular compartments (i.e., cytosol, cell membrane, nucleus, and mitochondria) and may impact multiple physiological processes (Singh, Pandey, Saha & Gattupalli, 2015; Stites et al., 2006). Previous studies attributed the biological role of PQQ to an increased expression of PGC-1α transcriptional coactivator. It was observed that PQQ activates PGC-1α promoter in Hepa 1–6 cell line due to elevated CREB phosphorylation at serine 133 and its binding to CRE site. As a consequence, 24 hr incubation with PQQ stimulated an increase in PGC-1α mRNA and protein content (+125% and +75%, respectively; Chowanadisai et al., 2010). Additionally, rats' treatment with bacterial strains containing an incorporated PQQ producing operon or dietary PQQ supplementation had elevated hepatic

PGC-1α mRNA level (+1.7-fold and +55%, respectively; Singh et al., 2015; Tchaparian et al., 2010). Herein, we provide evidence that PQQ significantly elevates PGC-1α content also in L6 myotubes in a dose- and time-dependent manner with the highest efficiency for 1 µM (transcript level) and 0.5 µM (protein level). Interestingly the observed changes in the coactivator mRNA and its transcript level did not exactly parallel each other (Figure 2). It seems that similar dissonance between the two was demonstrated in HepG2 cell line in response to PQQ treatment (Zhang et al., 2015). These results may suggest that, apart from CREB phosphorylation, also posttranscriptional regulation is engaged in PGC-1α expression modulation after PQQ administration. In fact, PQQ treatment of NIH/3T3 fibroblasts induced PGC-1α transcriptional activity by deacetylation of the protein as well as promoted its nuclear translocation (Saihara, Kamikubo, Ikemoto, Uchida & Akagawa, 2017). Moreover, PQQ treatment restored PGC-1α mRNA and protein level in the denervated murine gastrocnemius muscles, concomitantly with an increase in the expression of PGC-1α target genes (i.e., Tfam; Kuo, Shih, Kao, Yeh & Lee, 2015). A modest rate of PGC-1α upregulation achieved by using PQQ (protein level: +~20%) is of great importance, since massive (+6-fold) PGC-1α induction was related with elevated susceptibility to fat-induced muscle insulin resistance (Choi et al., 2008). It is also worth to emphasize that PGC-1α small interfering RNA transfection prevented the induction of mitochondrial biogenesis in PQQ-treated cells, as measured by citrate synthase (CS) activity and mitochondrial content (Chowanadisai et al., 2010). This strongly indicates that most of the effects exerted by PQQ treatment are mediated via PGC-1α. Consequently, PQQ activates about 2–4% of the total number of genes involved in mitochondrial biogenesis, cellular signaling pathways (Bauerly et al., 2011), immune and antioxidative responsiveness (Kumar & Kar, 2015; Rucker, Chowanadisai & Nakano, 2009), glucose tolerance (Takada et al., 2012), lipid peroxidation (Singh et al., 2015), and inflammatory processes (Harris et al., 2013). The above-mentioned processes remain also under strict control of PGC-1α (Eisele, Furrer, Beer & Handschin, 2015; Liang & Ward, 2006), thereby supporting a notion that PQQ actions are based predominantly on the stimulation of this coactivator (Eisele et al., 2015; Liang & Ward, 2006).

In relation to the influence of PQQ on palmitate uptake into skeletal muscle cells, we noticed a significant increase solely for prolonged treatment with 0.5 µM of PQQ. However, there are no literature data considering the impact of PQQ-mediated PGC-1α induction on changes in fatty acid uptake. Nevertheless, Espinoza, Boros, Crunkhorn, Gami, and Patti (2010) found that PGC-1α overexpression in C2C12 myotubes evoked only a small reduction in palmitic acid cellular import (−6%). Moreover, the rate of palmitic acid transport was almost unchanged (+9%) in L6 myotubes after PGC-1α downregulation (Lukaszuk, Miklosz, Chabowski & Gorski, 2015). We therefore suppose that in basal conditions PQQ/PGC-1α activation may exert relatively minor role in the uptake of fatty acids into muscle cells. Thus, the observed changes in intramyocellular lipid content would rather be a consequence of intrinsic metabolic changes evoked by PQQ, instead of fatty acid influx.

The presented results show a reduction in the intracellular pool of FFA paralleled by elevations in CER, SFO, and TAG levels, but
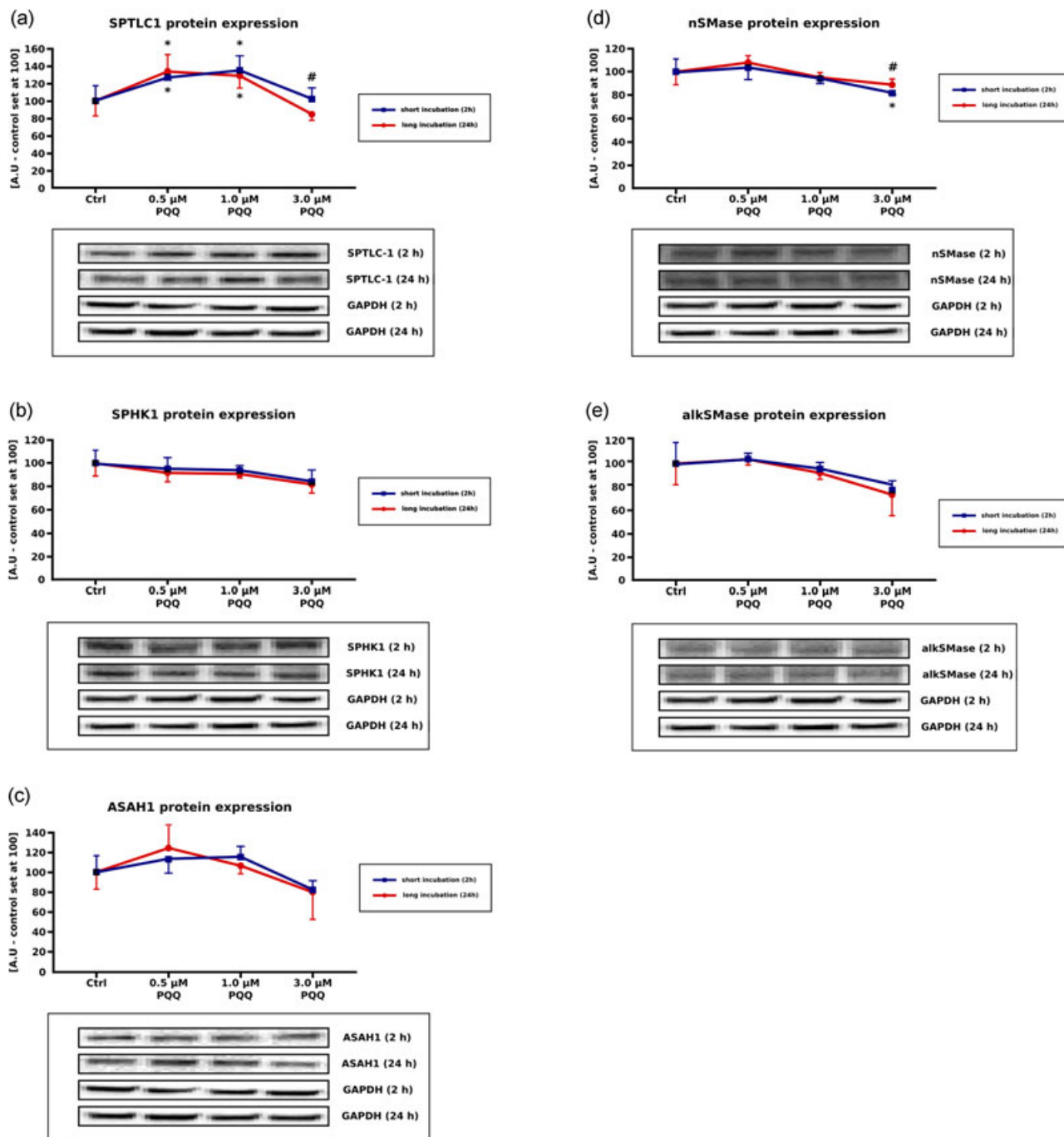
FIGURE 6 Effects of short- and long-term incubation with PQQ on sphingolipid metabolizing enzymes expression: SPT1 (a), ASAH1 (b), SPHK1 (c), N-SMase (d), and Alk-SMase (e) in L6 myotubes. Measurement of each treatment was taken as the average of six wells in the same experiments. Data are based on three independent determinations. Control is set as 100 and values are presented as mean ± SD. ANOVA with post hoc pairwise Student's t test (with Benjamini–Hochberg multiplicity correction). $*p < 0.05$, study group versus control; $\#p < 0.05$, long- vs. short-time incubation. Error bars (SD) are drawn in opposite directions to avoid overplotting. Alk-SMase: alkaline sphingomyelinase; ANOVA: analysis of variance; ASAH1: acidic ceramidase; N-SMase; neutral sphingomyelinase; PQQ: pyrroloquinoline quinone; SPT1: serine palmitoyltransferase 1; SPHK1: sphingosine kinase 1 [Color figure can be viewed at wileyonlinelibrary.com]

without a change in DAG amount. The above may imply a shift from FFA pool either into sphingolipid species or into TAG fraction. Accordingly, an increase in PGC-1α level (mRNA: +31%; protein: +20%) was accompanied by elevated TAG (+31%) content in skeletal muscle of lean Zucker rats (Benton et al., 2010). These changes could

be associated with the elevated expression of enzymes catalyzing two initial reactions in TAG synthesis, that is glycerophosphate acyltransferase (GPAT) and lysophosphatidic acid acyltransferase (LPAAT; Senoo et al., 2015), as well as fatty acid synthase (Benton et al., 2010). TAG storage, however, mimics the effect observed in

trained individuals, where it (TAG) serves as a "buffer" against lipotoxicity (Bergman et al., 2010). On the other hand, the unchanged DAG level in PGC-1α-overexpressing cells found confirmation in the results obtained from Zucker rats and TG mice (Benton et al., 2010; Liang et al., 2009). Similar changes in lipid profile of murine skeletal muscles were detected by Senoo et al. (2015), since PGC-1α overexpression increased TAG amount without affecting DAG level. Furthermore, especially for higher PQQ concentrations and the extended incubation time, an increase in the saturation status of TAG was not connected with an elevated unsaturated fatty acids level. These data may indicate the domination of β-oxidation of unsaturated fatty acids in mitochondria (Gaster, Rustan & Beck-Nielsen, 2005) or their redirection into other lipid fractions. Additionally, the elevated esterification of saturated fatty acids into TAG fraction may be a protective process, given that in cultured myotubes obtained from type 2 diabetic patients and in human individuals with type 2 diabetes the ability to store lipids in TAG pool is blunted (Sparks et al., 2014). Other studies, however, do not provide unambiguous evidence to confirm the alterations in myocellular lipid profile observed in our study. For instance, increased intramuscular lipid content in MPGC-1α TG mice has been demonstrated to originate from de novo lipogenesis connected with an enhancement in the level of both TAG and FFA in skeletal muscles (Summermatter, Baum, Santos, Hoppeler & Handschin, 2010). Instead, muscle-specific PGC-1α transfection was connected with a slightly elevated TAG level only in red, but not white muscle cells (Benton et al., 2008) so that the overall result may also be cellular-specific and depend on oxidative capacities.

Sphingolipids regulate numerous muscular biological processes, including contraction force, membrane excitability, regeneration, differentiation or growth, but also influence the rate of metabolic substrates usage by skeletal muscle cells (Bruni & Donati, 2008; Donati, Cencetti & Bruni, 2013; Nikolova-Karakashian & Reid, 2011). Selected sphingolipid classes often exert opposite effects so that their aberrant synthesis may induce pathological changes in skeletal muscles (i.e., oxidative stress, muscle fatigue, reduced glucose turnover, impaired satellite cells differentiation, or apoptosis; Nikolova-Karakashian & Reid, 2011). Consequently, pharmacological modulation of sphingolipids metabolism could be applied to prevention and therapy of many disorders. Nevertheless, previous study employing PGC-1α-knocked-down L6 myotubes did not show significant alterations in CER total content and composition (Lukaszuk et al., 2015). Moreover, the overexpression of PGC-1α in animal models (i.e., MPGC-1α TG and lean Zucker rats) did not produce changes in muscular CER level (Benton et al., 2010; Liang et al., 2009). On the contrary, in the present study the prolonged incubation (24 hr) with all the studied doses of PQQ (0.5, 1, 3 μM) enhanced CER level in L6 myotubes. Likewise, CER content (especially C16:0, C18:0, C18:1, and C18:2 moieties) was elevated in PGC-1α overexpressing C2C12 myotubes (Espinoza et al., 2010). Since the above-mentioned study and ours provided in vitro results, it is possible that the effects of PGC-1α action depend on extracellular milieu with a more pronounced impact towards lipid

accumulation during normal metabolic substrates provision (Espinoza et al., 2010). Additionally, in physiological in vivo conditions a compensatory activation of other mechanisms regulating sphingolipids metabolism may prevail. For instance, PGC-1α ablation may result in increased activity of other proteins from PGC-1 family, namely PGC-1β and PGC-1α-related coactivator (PRC), that partially overlap PGC-1α functions (Liu & Lin, 2011; Philp et al., 2011). However, data from skeletal muscle-restricted PGC-1α heterozygous mice did not confirm this assumption, since neither in skeletal muscles (i.e., gastrocnemius and soleus muscle), nor in other examined tissues (i.e., heart, liver, brain, and brown adipose tissue), the level of PGC-1β expression increased (Handschin et al., 2007). Similarly, physical exercise did not evoke compensatory enhancement in muscular PGC-1β level in muscle-specific PGC-1α null mice (Rowe, Jiang & Arany, 2010).

The observed increase in long-chain fatty acid species building CER molecules (i.e., C16:0, C18:0, and C18:1) in C2C12 cultured myotubes (Espinoza et al., 2010) resembles the effect observed with 0.5 μM of PQQ in this study. On the other hand, higher doses of PQQ were associated with slight decreases in C18:0-CER and C18:1-CER levels. It confirms that the rate of PGC-1α upregulation may be a crucial factor in the overall cellular response. Incubation with 0.5 μM of PQQ is also related with increased levels fatty acids (with carbon chain lengths: C20, C22, C24, and C24) composing CER. The accumulation of the above-mentioned CER building fatty acids was demonstrated to accompany insulin resistance and obesity (Adams et al., 2004). Furthermore, the observation that high rate of unsaturated fatty acids (i.e., C18:2 and C18:3) incorporation into CER fraction occurs in all the tested conditions may not necessarily be salutary. One report revealed that administration of conjugated linoleic acid and increased muscular CER content was connected with deteriorated insulin sensitivity in humans (Thrush et al., 2007). Therefore, the composition of CER, in addition to modulation of its total level, may play a key role when considering the effects of PGC-1α activation.

CER de novo synthesis proceeds through the activation of serine palmitoyltransferase, an endoplasmic reticulum-located enzyme that catalyzes the condensation of serine with palmitoyl-CoA (Figure 1). Our findings unveil that PQQ doses of 0.5 and 1 μM elevate SPT1 protein level, thereby implying activation of de novo CER formation. This seems to be additionally confirmed by the enhanced CER level observed in the cells incubated with 0.5 and 1 μM of PQQ (Figure 5c). This step is especially sensitive to changes in fatty acid availability and may be one of the reasons for the previously described decreased myocellular FFA content (Figure 4a). Interestingly, the impact of PQQ on specific sphingolipid metabolic pathways appears to be time-dependent since a decrease in SFA and SFA1P level was noticed after short-time exposure, while the salvage pathway was activated (i.e., elevated level of SFO) after prolonged treatment. Moreover, the observed alterations partially reflect exercise-mimicking effects of PGC-1α (Hoeks et al., 2012), since the induction of de novo CER synthesis combined with upregulated SFO content was noticed also in the

soleus and gastrocnemius muscles of rats after acute exercise (Dobrzyń & Górski, 2002).

To further explore the relationship between CER synthesis and PGC-1α stimulation in L6 myotubes, we evaluated the level of sphingomyelin, a major source of CER in stress conditions (Nikolova-Karakashian & Reid, 2011). In fact, we noticed a reduction in the total content of this compound for all of the applied PQQ doses, presumably as an effect of its (SM) shift toward CER formation. The concomitant decrease in sphingomyelin saturation status may impede its interactions with cholesterol and domain formation within biological membranes (Slotte & Ramstedt, 2007). However, whether PQQ actually influences the structural role of sphingomyelin remains to be established. In contrast, other researchers showed that PGC-1α overexpression in cultured C2C12 myotubes did not affect the content of C16:0, C18:0, C18:1, and C18:2 species in sphingomyelin, despite elevated CER level (Espinoza et al., 2010). Since there is no obvious explanation for these discrepancies, we may suspect that it is related with the level of PGC-1α overexpression (protein content: +20% in our study vs. +86-fold in the study by Espinoza et al., 2010) or with different strategies used to achieve the coactivator's upregulation (PQQ treatment in our research vs. adenoviral infection in the study by Espinoza et al., 2010).

To recapitulate, in the present study we used an inducible model of PGC-1α overexpression (i.e., 2 and 24 hr of PQQ treatment) to assess the changes in lipid profile of skeletal muscle L6 cells. The temporal PGC-1α upregulation confers a significant reduction in FFA level with simultaneous TAG and CER accumulations. It is also conceivable that the transient stimulation of PGC-1α may induce all three routs involved in CER production (i.e., de novo synthesis, salvage pathway, and sphingomyelin hydrolysis) in L6 myotubes depending on the dose and time of PQQ incubation. The provided results emphasize the role of PGC-1α in intramyocellular lipid turnover and its involvement in the esterification of fatty acids to specific lipid pools.

To sum up, the obtained data indicate a few phenomena occurring in response to PGC-1α stimulation. Importantly, we observed an increased content of TAG (in the range of +28–140%). This indicates a possible protective mechanism since TAG acts as a "buffer" against lipotoxicity. However, we found an elevated CER concentration, which could potentially disturb cellular signaling pathway (i.e., for insulin) in skeletal muscle cells. Nevertheless, we did not notice any accompanying changes in DAG level. The above-mentioned changes may be a kind of "beacon" signaling that further increase in PGC-1α protein expression, above the modest level, can be possibly harmful. In conclusion, data reported herein reinforce a role for PQQ/PGC-1α in lipid storage into CER and TAG lipid pools, in addition to an increment of cellular oxidative potential.

CONFLICTS OF INTEREST

The authors declare that there are no conflicts of interest.

AUTHOR CONTRIBUTIONS

E. S. designed and conducted research, wrote the manuscript; A. M. designed and conducted experiments, reviewed the manuscript; B. Ł. designed and conducted research, performed statistical analysis, reviewed the manuscript; A. C. revised final version of the manuscript.

ORCID

Agnieszka Mikłosz http://orcid.org/0000-0003-4936-3120
Bartłomiej Łukaszuk http://orcid.org/0000-0002-4954-3431

REFERENCES

Adams, J. M., Pratipanawatr, T., Berria, R., Wang, E., DeFronzo, R. A., Sullards, M. C. & Mandarino, L. J. (2004). Ceramide content is increased in skeletal muscle from obese insulin-resistant humans. *Diabetes*, 53(1), 25–31. https://doi.org/10.2337/DIABETES.53.1.25

Bauerly, K., Harris, C., Chowanadisai, W., Graham, J., Havel, P. J., Tchaparian, E., … Rucker, R. B. (2011). Altering pyrroloquinoline quinone nutritional status modulates mitochondrial, lipid, and energy metabolism in rats. *PLOS One*, 6(7), e21779. https://doi.org/10.1371/journal.pone.0021779

Benton, C. R., Holloway, G. P., Han, X.-X., Yoshida, Y., Snook, L. A., Lally, J., … Bonen, A. (2010). Increased levels of peroxisome proliferator-activated receptor gamma, coactivator 1 alpha (PGC-1α) improve lipid utilisation, insulin signalling and glucose transport in skeletal muscle of lean and insulin-resistant obese Zucker rats. *Diabetologia*, 53(9), 2008–2019. https://doi.org/10.1007/s00125-010-1773-1

Benton, C. R., Nickerson, J. G., Lally, J., Han, X.-X., Holloway, G. P., Glatz, J. F. C., … Bonen, A. (2008). Modest PGC-1alpha overexpression in muscle in vivo is sufficient to increase insulin sensitivity and palmitate oxidation in subsarcolemmal, not intermyofibrillar, mitochondria. *The Journal of Biological Chemistry*, 283(7), 4228–4240. https://doi.org/10.1074/jbc.M704332200

Bergman, B. C., Perreault, L., Hunerdosse, D. M., Koehler, M. C., Samek, A. M. & Eckel, R. H. (2010). Increased intramuscular lipid synthesis and low saturation relate to insulin sensitivity in endurance-trained athletes. *Journal of Applied Physiology (Bethesda, Md.: 1985)*, 108(5), 1134–1141. https://doi.org/10.1152/japplphysiol.00684.2009

Bligh, E. G. & Dyer, W. J. (1959). A rapid method of total lipid extraction and purification. *Canadian Journal of Biochemistry and Physiology*, 37(8), 911–917. https://doi.org/10.1139/o59-099

Bruni, P. & Donati, C. (2008). Pleiotropic effects of sphingolipids in skeletal muscle. *Cellular and Molecular Life Sciences*, 65(23), 3725–3736. https://doi.org/10.1007/s00018-008-8236-6

Chavez, J. A. & Summers, S. A. (2003). Characterizing the effects of saturated fatty acids on insulin signaling and ceramide and diacylglycerol accumulation in 3T3-L1 adipocytes and C2C12 myotubes. *Archives of Biochemistry and Biophysics*, 419(2), 101–109. Retrieved from. http://www.ncbi.nlm.nih.gov/pubmed/14592453

Choi, C. S., Befroy, D. E., Codella, R., Kim, S., Reznick, R. M., Hwang, Y.-J., … Shulman, G. I. (2008). Paradoxical effects of increased expression of

PGC-1alpha on muscle mitochondrial function and insulin-stimulated muscle glucose metabolism. *Proceedings of the National Academy of Sciences of the United States of America*, *105*(50), 19926–19931. https://doi.org/10.1073/pnas.0810339105

Chowanadisai, W., Bauerly, K. A., Tchaparian, E., Wong, A., Cortopassi, G. A. & Rucker, R. B. (2010). Pyrroloquinoline quinone stimulates mitochondrial biogenesis through cAMP response element-binding protein phosphorylation and increased PGC-1alpha expression. *The Journal of Biological Chemistry*, *285*(1), 142–152. https://doi.org/10.1074/jbc.M109.030130

Christie, W. W. (1982). A simple procedure for rapid transmethylation of glycerolipids and cholesteryl esters. *Journal of Lipid Research*, *23*(7), 1072–1075. Retrieved from. http://www.ncbi.nlm.nih.gov/pubmed/6897259

Dobrzyń, A. & Górski, J. (2002). Effect of Acute Exercise on the Content of Free Sphinganine and Sphingosine in Different Skeletal Muscle Types of the Rat. *Hormone and Metabolic Research*, *34*(9), 523–529. https://doi.org/10.1055/s-2002-34793

Donati, C., Cencetti, F. & Bruni, P. (2013). Sphingosine 1-phosphate axis: A new leader actor in skeletal muscle biology. *Frontiers in Physiology*, *4*, 338. https://doi.org/10.3389/fphys.2013.00338

Eisele, P. S., Furrer, R., Beer, M. & Handschin, C. (2015). The PGC-1 coactivators promote an anti-inflammatory environment in skeletal muscle in vivo. *Biochemical and Biophysical Research Communications*, *464*(3), 692–697. https://doi.org/10.1016/j.bbrc.2015.06.166

Espinoza, D. O., Boros, L. G., Crunkhorn, S., Gami, H. & Patti, M. E. (2010). Dual modulation of both lipid oxidation and synthesis by peroxisome proliferator-activated receptor- coactivator-1 and -1 in cultured myotubes. *The FASEB Journal*, *24*(4), 1003–1014. https://doi.org/10.1096/fj.09-133728

Frontera, W. R. & Ochala, J. (2015). Skeletal Muscle: A Brief Review of Structure and Function. *Calcified Tissue International*, *96*(3), 183–195. https://doi.org/10.1007/s00223-014-9915-y

Gaster, M., Rustan, A. C. & Beck-Nielsen, H. (2005). Differential utilization of saturated palmitate and unsaturated oleate: Evidence from cultured myotubes. *Diabetes*, *54*(3), 648–656. Retrieved from. http://www.ncbi.nlm.nih.gov/pubmed/15734839

Handschin, C., Choi, C. S., Chin, S., Kim, S., Kawamori, D., Kurpad, A. J., ... Spiegelman, B. M. (2007). Abnormal glucose homeostasis in skeletal muscle-specific PGC-1alpha knockout mice reveals skeletal muscle-pancreatic beta cell crosstalk. *The Journal of Clinical Investigation*, *117*(11), 3463–3474. https://doi.org/10.1172/JCI31785

Harris, C. B., Chowanadisai, W., Mishchuk, D. O., Satre, M. A., Slupsky, C. M. & Rucker, R. B. (2013). Dietary pyrroloquinoline quinone (PQQ) alters indicators of inflammation and mitochondrial-related metabolism in human subjects. *The Journal of Nutritional Biochemistry*, *24*(12), 2076–2084. https://doi.org/10.1016/j.jnutbio.2013.07.008

He, K., Nukada, H., Urakami, T. & Murphy, M. P. (2003). Antioxidant and pro-oxidant properties of pyrroloquinoline quinone (PQQ): Implications for its function in biological systems. *Biochemical Pharmacology*, *65*(1), 67–74. Retrieved from. http://www.ncbi.nlm.nih.gov/pubmed/12473380

Hoeks, J., Arany, Z., Phielix, E., Moonen-Kornips, E., Hesselink, M. K. C. & Schrauwen, P. (2012). Enhanced lipid-but not carbohydrate-supported mitochondrial respiration in skeletal muscle of PGC-1α overexpressing mice. *Journal of Cellular Physiology*, *227*(3), 1026–1033. https://doi.org/10.1002/jcp.22812

Kumar, N. & Kar, A. (2015). Pyrroloquinoline quinone (PQQ) has potential to ameliorate streptozotocin-induced diabetes mellitus and oxidative stress in mice: A histopathological and biochemical study. *Chemico-Biological Interactions*, *240*, 278–290. https://doi.org/10.1016/j.cbi.2015.08.027

Kuo, Y.-T., Shih, P.-H., Kao, S.-H., Yeh, G.-C. & Lee, H.-M. (2015). Pyrroloquinoline quinone resists denervation-induced skeletal muscle atrophy by activating PGC-1α and integrating mitochondrial electron transport chain complexes. *PLOS One*, *10*(12), e0143600. https://doi.org/10.1371/journal.pone.0143600

Liang, H., Balas, B., Tantiwong, P., Dube, J., Goodpaster, B. H., O'Doherty, R. M., ... Ward, W. F. (2009). Whole body overexpression of PGC-1α has opposite effects on hepatic and muscle insulin sensitivity. *American Journal of Physiology-Endocrinology and Metabolism*, *296*(4), E945–E954. https://doi.org/.org/10.1152/ajpendo.90292.2008

Liang, H. & Ward, W. F. (2006). PGC-1α: A key regulator of energy metabolism. *Advances in Physiology Education*, *30*, 4–151.

Lipina, C. & Hundal, H. S. (2017). Lipid modulation of skeletal muscle mass and function. *Journal of Cachexia, Sarcopenia and Muscle*, *8*(2), 190–201. https://doi.org/10.1002/jcsm.12144

Lira, V. A., Benton, C. R., Yan, Z. & Bonen, A. (2010). PGC-1alpha regulation by exercise training and its influences on muscle function and insulin sensitivity. *American Journal of Physiology Endocrinology and Metabolism*, *299*(2), E145–E161. https://doi.org/10.1152/ajpendo.00755.2009

Liu, C. & Lin, J. D. (2011). PGC-1 coactivators in the control of energy metabolism. *Acta Biochimica et Biophysica Sinica*, *43*(4), 248–257. https://doi.org/10.1093/abbs/gmr007

Lukaszuk, B., Miklosz, A., Chabowski, A. & Górski, J. (2015). Modest decrease in Pgc1a results in TAG accumulation but not in insulin resistance in L6 myotubes. *Cellular Physiology and Biochemistry*, *35*(4), 1609–1622. https://doi.org/10.1159/000373975

Mahadevappa, V. G. & Holub, B. J. (1987). Quantitative loss of individual eicosapentaenoyl-relative to arachidonoyl-containing phospholipids in thrombin-stimulated human platelets. *Journal of Lipid Research*, *28*(11), 1275–1280. Retrieved from. http://www.ncbi.nlm.nih.gov/pubmed/2828497

Mikłosz, A., Łukaszuk, B., Baranowski, M., Górski, J. & Chabowski, A. (2013). Effects of inhibition of serine palmitoyltransferase (SPT) and sphingosine kinase 1 (SphK1) on palmitate induced insulin resistance in L6 myotubes. *PLOS One*, *8*(12), e85547. https://doi.org/10.1371/journal.pone.0085547

Mikłosz, A., Łukaszuk, B., Żendzian-Piotrowska, M., Brańska-Januszewska, J., Ostrowska, H. & Chabowski, A. (2017). Challenging of AS160/TBC1D4 alters intracellular lipid milieu in L6 myotubes incubated with palmitate. *Journal of Cellular Physiology*, *232*(9), 2373–2386.

Mikłosz, A., Łukaszuk, B., Żendzian-Piotrowska, M., Kurek, K., Chabowski, A. (2016). The effects of AS160 modulation on fatty acid transporters expression and lipid profile in L6 myotubes. *Cell Physiol Biochem*, *38*(1), 267–282.

Morrison, W. R. & Smith, L. M. (1964). Preparation of fatty acid methyl esters and dimethylacetals from lipids with boron fluoride—methanol. *Journal of Lipid Research*, *5*, 600–608. Retrieved from. http://www.ncbi.nlm.nih.gov/pubmed/14221106

Naito, Y., Kumazawa, T., Kino, I. & Suzuki, O. (1993). Effects of pyrroloquinoline quinone (PQQ) and PQQ-oxazole on DNA synthesis of cultured human fibroblasts. *Life Sciences*, *52*(24), 1909–1915. https://doi.org/10.1016/0024-3205(93)90631-C

Nikolova-Karakashian, M. N. & Reid, M. B. (2011). Sphingolipid metabolism, oxidant signaling, and contractile function of skeletal muscle. *Antioxidants & Redox Signaling*, *15*(9), 2501–2517. https://doi.org/10.1089/ars.2011.3940

Pfaffl, M. W. (2001). A new mathematical model for relative quantification in real-time RT-PCR. *Nucleic Acids Research*, *29*(9), e45–e45. Retrieved from. http://www.ncbi.nlm.nih.gov/pubmed/11328886

Philp, A., Belew, M. Y., Evans, A., Pham, D., Sivia, I., Chen, A., ... Baar, K. (2011). The PGC-1α-related coactivator promotes mitochondrial and myogenic adaptations in C2C12 myotubes. *American Journal of Physiology-Regulatory, Integrative and Comparative Physiology*, *301*(4), R864–R872. https://doi.org/10.1152/ajpregu.00232.2011

Rowe, G. C., Jiang, A. & Arany, Z. (2010). PGC-1 coactivators in cardiac development and disease. *Circulation Research*, *107*(7), 825–838. https://doi.org/10.1161/CIRCRESAHA.110.223818

Rucker, R., Chowanadisai, W. & Nakano, M. (2009). Potential physiological importance of pyrroloquinoline quinone. *Alternative Medicine Review: A*

Journal of Clinical Therapeutic, 14(3), 268–277. Retrieved from. http://www.ncbi.nlm.nih.gov/pubmed/19803551

Saihara, K., Kamikubo, R., Ikemoto, K., Uchida, K. & Akagawa, M. (2017). Pyrroloquinoline quinone, a redox-active *o*-quinone, stimulates mitochondrial biogenesis by activating the SIRT1/PGC-1α signaling pathway. *Biochemistry*, 56(50), 6615–6625. https://doi.org/10.1021/acs.biochem.7b01185

Samovski, D., Su, X., Xu, Y., Abumrad, N. A. & Stahl, P. D. (2012). Insulin and AMPK regulate FA translocase/CD36 plasma membrane recruitment in cardiomyocytes via Rab GAP AS160 and Rab8a Rab GTPase. *Journal of Lipid Research*, 53(4), 709–717. https://doi.org/10.1194/jlr.M023424

Senoo, N., Miyoshi, N., Goto-Inoue, N., Minami, K., Yoshimura, R., Morita, A., … Miura, S. (2015). PGC-1α-mediated changes in phospholipid profiles of exercise-trained skeletal muscle. *Journal of Lipid Research*, 56(12), 2286–2296. https://doi.org/10.1194/jlr.M060533

Singh, A. K., Pandey, S. K., Saha, G. & Gattupalli, N. K. (2015). Pyrroloquinoline quinone (PQQ) producing *Escherichia coli* Nissle 1917 (EcN) alleviates age associated oxidative stress and hyperlipidemia, and improves mitochondrial function in ageing rats. *Experimental Gerontology*, 66, 1–9. https://doi.org/10.1016/j.exger.2015.04.001

Sitnick, M. T., Basantani, M. K., Cai, L., Schoiswohl, G., Yazbeck, C. F., Distefano, G., … Kershaw, E. E. (2013). Skeletal muscle triacylglycerol hydrolysis does not influence metabolic complications of obesity. *Diabetes*, 62(10), 3350–3361. https://doi.org/10.2337/db13-0500

Slotte, J. P. & Ramstedt, B. (2007). The functional role of sphingomyelin in cell membranes. *European Journal of Lipid Science and Technology*, 109(10), 977–981. https://doi.org/10.1002/ejlt.200700024

Smidt, C. R., Unkefer, C. J., Houck, D. R. & Rucker, R. B. (1991). Intestinal absorption and tissue distribution of [^{14}C]pyrroloquinoline quinone in mice. *Society for Experimental Biology and Medicine (New York, N.Y.)*, 197(1), 27–31. Retrieved from. http://www.ncbi.nlm.nih.gov/pubmed/1850522

Smith, M. E., Tippetts, T. S., Brassfield, E. S., Tucker, B. J., Ockey, A., Swensen, A. C., … Bikman, B. T. (2013). Mitochondrial fission mediates ceramide-induced metabolic disruption in skeletal muscle. *Biochemical Journal*, 456(3), 427–439. https://doi.org/10.1042/BJ20130807

Sparks, L. M., Bosma, M., Brouwers, B., van de Weijer, T., Bilet, L., Schaart, G., … Schrauwen, P. (2014). Reduced incorporation of fatty acids into triacylglycerol in myotubes from obese individuals with type 2 diabetes. *Diabetes*, 63(5), 1583–1593. https://doi.org/10.2337/db13-1123

Stites, T., Storms, D., Bauerly, K., Mah, J., Harris, C., Fascetti, A., … Rucker, R. B. (2006). Pyrroloquinoline quinone modulates mitochondrial quantity and function in mice. *The Journal of Nutrition*, 136(2), 390–396. https://doi.org/10.1093/jn/136.2.390

Summermatter, S., Baum, O., Santos, G., Hoppeler, H. & Handschin, C. (2010). Peroxisome proliferator-activated receptor {gamma} coactivator 1{alpha} (PGC-1{alpha}) promotes skeletal muscle lipid refueling in vivo by activating de novo lipogenesis and the pentose phosphate pathway. *The Journal of Biological Chemistry*, 285(43), 32793–32800. https://doi.org/10.1074/jbc.M110.145995

Supruniuk, E., Mikłosz, A. & Chabowski, A. (2017). The Implication of PGC-1α on Fatty Acid Transport across Plasma and Mitochondrial Membranes in the Insulin Sensitive Tissues. *Frontiers in Physiology*, 8, 923. https://doi.org/10.3389/fphys.2017.00923

Takada, M., Sumi, M., Maeda, A., Watanabe, F., Kamiya, T., Ishii, T., … Akagawa, M. (2012). Pyrroloquinoline quinone, a novel protein tyrosine phosphatase 1B inhibitor, activates insulin signaling in C2C12 myotubes and improves impaired glucose tolerance in diabetic KK-Ay mice. *Biochemical and Biophysical Research Communications*, 428(2), 315–320. https://doi.org/10.1016/j.bbrc.2012.10.055

Tchaparian, E., Marshal, L., Cutler, G., Bauerly, K., Chowanadisai, W., Satre, M., … Rucker, R. B. (2010). Identification of transcriptional networks responding to pyrroloquinoline quinone dietary supplementation and their influence on thioredoxin expression, and the JAK/STAT and MAPK pathways. *Biochemical Journal*, 429(3), 515–526. https://doi.org/10.1042/BJ20091649

Thrush, A. B., Chabowski, A., Heigenhauser, G. J., McBride, B. W., Or-Rashid, M. & Dyck, D. J. (2007). Conjugated linoleic acid increases skeletal muscle ceramide content and decreases insulin sensitivity in overweight, non-diabetic humans. *Applied Physiology, Nutrition, and Metabolism*, 32(3), 372–382. https://doi.org/10.1139/H06-116

Watt, M. J. & Hoy, A. J. (2012). Lipid metabolism in skeletal muscle: Generation of adaptive and maladaptive intracellular signals for cellular function. *American Journal of Physiology-Endocrinology and Metabolism*, 302(11), E1315–E1328. https://doi.org/10.1152/ajpendo.00561.2011

Yang, C., Yu, L., Kong, L., Ma, R., Zhang, J., Zhu, Q., … Hao, D. (2014). Pyrroloquinoline quinone (PQQ) inhibits lipopolysaccharide induced inflammation in part via downregulated NF-κB and p38/JNK activation in microglial and attenuates microglia activation in lipopolysaccharide treatment mice. *PLOS One*, 9(10), e109502. https://doi.org/10.1371/journal.pone.0109502

Zhang, J., Meruvu, S., Bedi, Y. S., Chau, J., Arguelles, A., Rucker, R. & Choudhury, M. (2015). Pyrroloquinoline quinone increases the expression and activity of Sirt1 and -3 genes in HepG2 cells. *Nutrition Research*, 35(9), 844–849. https://doi.org/10.1016/j.nutres.2015.06.014